

The Nainital-Cape Survey-IV

Santosh Joshi¹, P. Martinez^{2,3}, Sowgata Chowdhury^{1,4}, N. K. Chakradhari⁵, Y. C. Joshi¹, P. van Heerden³,
T. Medupe⁶, Yerra Bharat Kumar⁷, R. B. Kuhn³

¹ Aryabhata Research Institute of Observational Sciences, Manora peak, Nainital-263129, India
e-mail: santosh@aries.res.in

² SpaceLab, Department of Electrical Engineering, University of Cape Town, Private Bag X3, Rondebosch 7701, South Africa

³ South African Astronomical Observatory, P.O. Box 9, Observatory 7935, South Africa

⁴ Department of Physics, Christ University, Hosur Road, Bangalore - 560029, Karnataka, India

⁵ School of Studies in Physics and Astrophysics, Pt Ravishankar Shukla University, Raipur 492 010, India

⁶ Department of Physics, University of the North-West, Private Bag X2046, Mmabatho 2735, South Africa

⁷ National Astronomical Observatories, Chinese Academy of Sciences, 20A Datun Road, Chaoyang District, Beijing, China

Received; accepted

ABSTRACT

Context. The Nainital-Cape survey is a dedicated ongoing survey programme to search for and study pulsational variability in chemically peculiar (CP) stars to understand their internal structure and evolution.

Aims. The main aims of this survey are to find new pulsating Ap and Am stars in the northern and southern hemisphere and to perform asteroseismic studies of these new pulsators.

Methods. The survey is conducted using high-speed photometry. The candidate stars were selected on the basis of having Strömgren photometric indices similar to those of known pulsating CP stars.

Results. Over the last decade a total of 337 candidate pulsating CP stars were observed for the Nainital-Cape survey, making it one of the longest ground-based surveys for pulsation in CP stars in terms of time span and sample size. The previous papers of this series presented seven new pulsating variables and 229 null results. In this paper we present the light curves, frequency spectra and the various astrophysical parameters of the 108 additional CP stars observed since the last reported results. We have also tabulated the basic physical parameters of the known roAp stars. As part of establishing the detection limits in the Nainital-Cape survey, we investigated the scintillation noise level at the two observing sites used in this survey, Sutherland and Nainital, by comparing the combined frequency spectra stars observed from each location. Our analysis shows that both the sites permit the detection of variations on the order of 0.6 milli-magnitude (mmag) in the frequency range 1-4 mHz, with Sutherland being marginally better, on average.

Key words. stars : chemically peculiar - stars : oscillations - variables : roAp : variable : δ -Scuti - survey : catalogue

1. Introduction

A chemically peculiar (CP) star can be distinguished from a chemically normal star by its spectrum, where anomalies can be seen on a visual inspection of low-dispersion spectra. The optical spectra of the CP stars exhibit normal hydrogen lines combined with enhanced silicon, metal, and/or rare-earth lines and weak calcium lines. The chemical peculiarities in these stars result from the diffusion process (Michaud 1970; Michaud et al. 1981; Babel 1992; Richer et al. 2000). Chemical elements with many lines near flux maximum, such as iron peak and rare earth elements, are brought up to the surface by the dominance of radiation pressure over gravity in the radiative envelopes of these stars, causing an apparent over-abundance of such elements. The elements with few lines near the flux maximum settle gravitationally and appear to be under-abundant. Slow rotation is thus a basic condition to operate the diffusion process in CP stars. The CP stars are found on the main-sequence between spectral types B2 and F5, from the zero-age main-sequence (ZAMS) to the terminal-age main-sequence (TAMS), and have masses ranging from 1.5 to about $7 M_{\odot}$.

Based on their spectroscopic characteristics, Preston (1974) divided the CP stars into following groups : Am/Fm (CP1),

Ap/Bp (CP2), Hg-Mn (CP3), He weak and He strong (CP4) stars. Renson & Manfroid (2009) compiled an up-to-date catalogue of 8205 CP stars. A subset of Ap and Am stars shows photometric variability with periods ranging from a few minutes to a few hours, and are the focus of the Nainital - Cape survey.

The Am/Fm stars are relatively cool stars of spectral type F5-A8, with temperatures ranging from 6500 K to 10000 K. The spectra of these stars exhibit an under-abundance (weak lines) of Ca or Sc (or of both elements) and over-abundance (strong lines) of Sr, Eu and other rare-earth elements. Some of the members of this group show δ Sct-type pulsational variability (Joshi et al. 2003, 2006, 2009; Smalley et al. 2011; Catanzaro & Ripepi 2014; Hou et al. 2015). The Am stars rotate slower than chemically normal A-type stars and the frequency of binarity among these stars is much higher than among normal stars of the same mass (Abt & Golson 1962, Abt & Snowden 1973). It is well understood that these stars do not exhibit strong global magnetic fields, however based on the observations from Kepler space mission, Balona et al. (2015) found flares in two Am stars, which strongly suggests that at least some Am stars possess the significant magnetic fields.

The Ap/Bp stars have effective temperatures in the range of 6400 K to 15000 K. These stars exhibit the most conspicuous chemical anomalies of all the CP stars: enhanced lines of some elements, particularly Si, Cr, Sr, Mn, Fe, Eu, Gd, and Ce (over-

abundant by up to a factor of 10^6), and weak lines of light elements (under-abundant by a factor of 10^{-2}). The Ap stars show low rotation velocities with $v_e \sin i$ usually not exceeding 100 km s^{-1} . These stars have strong global magnetic fields with an intensity ranging from hundreds of gauss to tens of kilogauss.

The coolest sub-group of Ap stars ($6400 \text{ K} \leq T_{\text{eff}} \leq 8700 \text{ K}$) located near the main-sequence (MS) part of the classical instability strip, are known as roAp stars. Since the discovery of first roAp star HD 101065 (Kurtz 1978), 61 other members of this class have been discovered (Smalley et al. 2015). The roAp stars show pulsational variability in both the broad photometric bands and in narrow spectral lines. These pulsations are characterized as high-overtone, low-degree p -modes with typical periods between 5.6 min and 23.6 min and photometric amplitudes ranging from a few micro-magnitudes (μmag) up to tens of milli-magnitudes (mmag) and radial velocity (RV) amplitudes ranging from a few ms^{-1} to kms^{-1} . The roAp stars possess strong magnetic fields with typical strengths of a few kG to tens of kG (Hubrig et al. 2012) with over-abundances of some rare earth elements that can exceed the solar value by 10^6 (Ryabchikova et al. 2004). To date, there have been no roAp stars found in close binary systems though a few Ap stars are in close binaries. The roAp stars are among the more challenging MS stars to model due to their pulsations in the combined presence of a strong global magnetic field together with element segregation and stratification, but at the same time they can be considered as a stellar atomic physics laboratory.

The pulsation frequency spectrum of some of the roAp stars shows frequency multiplets with spacings corresponding to the frequency of rotation of the star. This phenomenon can be explained using the oblique pulsator model (Kurtz 1982), in which the pulsation axis is aligned with the axis of the magnetic field, which is assumed to be roughly a dipole inclined with respect to the axis of rotation. As a star rotates, the observed aspect of the pulsation changes, leading to amplitude modulation and, in some cases, phase modulation. The driving mechanism of the pulsations in roAp stars is thought to be the classical κ -mechanism operating in the partial hydrogen ionization zone (Balmforth et al. 2001). Cunha & Gough (2001) suggested an alternative excitation mechanism for roAp stars where pulsation is driven by the turbulent pressure in the convection zone.

Some roAp stars have highly stable pulsation frequencies and amplitudes, even on time scales of years while other roAp stars show frequency and amplitude variations on time scales as short as hours (Medupe et al. 2015). Whether this is a result of driving and damping, mode coupling or some instability is not known. It is important to know where in the roAp instability strip the stable and unstable pulsators lie.

The Kepler mission, launched in 2009 with the aim to detect and characterize Earth-sized planets in the habitable zone, has revolutionized our ability to detect and study very low-amplitude light variations of the order of a few $\mu\text{-mag}$ in rather faint stars (Koch et al. 2010). The Kepler mission has enabled the discovery of five roAp stars, all which have pulsation amplitudes much below the detection limits of ground-based photometry.

While initially roAp stars were discovered and studied with photometric methods, time-resolved spectroscopy has allowed the study of wider physical aspects of the pulsating stellar atmosphere. The rapid radial velocity variations of spectral lines of certain chemical elements allow us to sample the velocity field in the stellar atmosphere as a function of atmospheric depth. Of the 61 known roAp stars, about a quarter of them were discovered using spectroscopic methods. A combination of simultaneous spectroscopy and photometry constitutes the most sophis-

ticated asteroseismic data set for any roAp star. The observed phase lag between the variations in luminosity and in RV is an important parameter for modeling the stellar structure.

Similar to other pulsating stars, the roAp stars are also excellent asteroseismic candidates through which one can compare the observed frequency spectrum to the asymptotic pulsation theory and then obtain information about the spherical harmonic degrees of the pulsation modes, the distortion of the modes from normal modes, atmospheric structures, evolutionary status and the geometry of the magnetic field. Using such information one can derive the various physical parameters such as rotation periods, temperatures, luminosities, radii and their masses (see Joshi & Joshi (2015) for a recent review on asteroseismology of pulsating stars). Although the extent of the roAp phenomenon has been fairly well delineated in photometric and spectroscopic terms, there is as yet no known combination of these (and other) observable parameters that can be used as a predictor of pulsation in any given Ap star. In other words, one can have two Ap stars that are apparently similar in all observable parameters, where one is a pulsating roAp star and the other has no detectable pulsations and is a so-called “noAp” star.

The Nainital-Cape survey was initiated in 1999 by the Aryabhata Research Institute of Observational Sciences (ARIES) at Manora Peak, Nainital, India, and the South African Astronomical Observatory (SAAO) in Sutherland to search for pulsations in CP stars. The goals of the survey were: (i) to increase the number of known pulsating CP stars; (ii) to determine the observational limits of the roAp phenomenon; and (iii) to broaden the number and distribution (in parameter space) of established constant (noAp) stars, so as to shed some light on what distinguishes the pulsating from the apparently constant CP stars of similar spectral type and other observable physical parameters. This is the only survey of its kind which was conducted from both the northern and southern hemisphere. The first three papers of this survey described the scope and methods of the survey and reported the discovery of pulsations in several CP stars (Martinez et al. 2001; Paper-I, Joshi et al. 2006; Paper-II, Joshi et al. 2009; Paper-III). The present paper is the fourth in this series and presents the null results obtained for 108 stars observed during the period of 2006 to 2009.

Similar to other papers of this series, the present paper is also based on photoelectric photometry of the sample stars and is organized as follows: the target selection, observations and data reduction procedures are described in Section 2, followed by the frequency analysis of the time series photometric data in Section 3. In Sec. 4, the observational limits for the detection of light variations at the ARIES and SAAO sites are discussed. The stars classified as null results and their basic astrophysical parameters are given in Sec. 5. In Sec. 6, we provide the basic physical parameters of all the currently known roAp stars. In this section, we also compare the evolutionary status of the known roAp stars to the sample of stars observed under the Nainital-Cape survey. The statistics of several surveys to search for new roAp stars are discussed in Sec. 8. Finally, we outline the conclusions drawn from our study in Sec. 9.

2. Target Selection, Observations and Data Reduction

2.1. Selection Criteria

Following the target selection strategy of Martinez et al. (1991), the primary source of candidates for the Nainital-Cape survey was the subset of CP stars with Strömgren photometric indices

similar to those of the known roAp stars. In this range, we have also found many Am stars and included them in the list of targets. Apart from the sources of target mentioned in Martinez et al. (1991), we also included Ap/Am stars from Renson et al. (1991) and magnetic stars from Bychkov et al. (2003).

On the basis of the Strömgren photometric indices of known roAp stars (see Table 1), we have revised the range of indices that encompass the roAp phenomenon:

$$\begin{aligned} 0.082 &\leq b - y \leq 0.431 \\ 0.178 &\leq m_1 \leq 0.387 \\ -0.204 &\leq \delta m_1 \leq 0.012 \\ 0.002 &\leq c_1 \leq 0.870 \\ -0.370 &\leq \delta c_1 \leq 0.031 \\ 2.64 &\leq \beta \leq 2.88 \end{aligned}$$

where $b - y$ is the color index and β measures the strength of the H_β line, which is indicator of temperature for stars in the spectral range from around A3 to F2. The m_1 and c_1 indices indicate enhanced metallicity and increased line blanketing, respectively. The parameters δm_1 and δc_1 measure the blanketing difference and Balmer discontinuity relative to the ZAMS for a given β , respectively. Indices in the ranges given above are not an unambiguous indicator of roAp pulsation, although they serve to narrow down the field of candidates to the most promising subset. It is interesting to note that, whereas previously the roAp phenomenon seemed to be confined to the temperature range of the δ Scuti instability strip, it now appears that the roAp instability strip has a considerably cooler red edge, well into the F-type stars (see Fig. 2). As can be seen by the paucity of cooler stars tested for pulsation, this is an area for future work, to establish more firmly the cool edge of the roAp instability strip.

2.2. Photometric Observations

For many roAp stars, the pulsational photometric variations have amplitudes less than twenty mmag. The detection of such low-amplitude variations demands high-precision photometric observations that can be attained with fast photometers mounted on small telescopes at observing sites such as ARIES Nainital in India and SAAO Sutherland South Africa. The ARIES observations presented in this paper were acquired using the ARIES high-speed photoelectric photometer (Ashoka et al. 2001) attached to the 1.04-m Sampurnanand telescope at ARIES. The SAAO observations were acquired using the Modular Photometer attached to the 0.5-m telescope and the University of Cape Town photometer attached to the 0.75-m and 1.0-m telescopes at the Sutherland site of SAAO.

Each star was observed in high-speed photometric mode with continuous 10-sec integrations through a Johnson B filter. The observations were acquired in a single-channel mode (i.e. no simultaneous comparison star observations), with occasional interruptions to measure the sky background, depending on the phase and position of the moon. To minimize the effects of seeing fluctuations and tracking errors, we selected a photometric aperture of $30''$. Each target was observed continuously for 1-3 hours at a time. Since the amplitudes of the rapid photometric oscillations in roAp stars exhibit modulation due to rotation and also due to interference among frequencies of different pulsation modes, a null detection for pulsation may be obtained simply due to a coincidence of the timing of the observations. Hence, each candidate was observed several times.

2.3. Data Reduction

The data reduction process began with a visual inspection of the light curve to identify and remove obviously bad data points, followed by correction for coincidence counting losses, subtraction of the interpolated sky background, and correction for the mean atmospheric extinction. After applying these corrections, the time of the mid-point of the each observation was converted into a heliocentric Julian date (HJD) with an accuracy of 10^{-5} day (~ 1 sec). The reduced data comprise a time-series of HJD and ΔB magnitude with respect to the mean of the light curve.

3. Frequency Analysis

A fast algorithm (Kurtz 1985) based on Deeming's discrete Fourier transform (DFT) for unequally spaced data (Deeming 1975) was used to calculate the Fourier Transformation. The light curves were also inspected visually for evidence of δ Sct oscillations with periods of a few tens of minutes and longer. On these time-scales, single-channel photometric data are affected by sky transparency variations and it is not always possible to distinguish between oscillations in the star and variations in sky transparency. This is where the comparison of data of the same star acquired under different conditions on different nights is helpful for confirming the tentative detection of coherent oscillations in a given light curve.

After visual inspection of the light curves to search for indications of δ Sct pulsations in a given light curve on time-scales longer than about half an hour, we removed the sky transparency variations from the DFT data in order to reduce the overall noise level to approximately the scintillation noise. This is practicable for single-channel data because, on good photometric nights, the roAp oscillation frequencies are generally well resolved from the sky transparency variations. To remove the effect of sky transparency variations, the DFT data were prewhitened to remove signals with frequencies in the range 0 – 0.9 mHz, which is the frequency range commonly affected by sky transparency variations in single-channel photometric data. These frequencies were removed one at a time until the noise level in the DFT of the residuals approximated a white noise spectrum. Depending on the stability of the photometric transparency of a given night, it was generally possible to correct for the effects of sky transparency by removing 3-5 frequencies in the above-mentioned frequency range.

The first and second panels of Fig. 3 show the light curves of the candidate stars filtered for low-frequency sky transparency variations. The third and fourth panels show the pre-whitened amplitude spectra of the sample stars filtered for low-frequency sky transparency variations.

4. Noise Level Characterization

The detection limit for photometric variability depends upon the atmospheric noise, which consists of scintillation noise and sky-transparency variations, and the photon noise. For the brighter (~ 10 mag) stars, the atmospheric scintillation noise dominates over the photon noise and is one of the fundamental factors limiting the precision of ground-based photometry. In order to characterize the two observing sites used in the Nainital-Cape survey and to put constraints on the detection limits for low-amplitude variability, we estimated the observational as well as the theoretical scintillation noise values for both the sites.

Given a telescope's altitude, mirror diameter, and the observational exposure time and airmass, one can find the contribu-

tion of scintillation noise in photometric measurements using Young's approximation (Young 1967, 1974). Using this scaling relation, it is possible to compare the level of scintillation noise at different observatory sites. Although the precise amount of scintillation changes from night to night, Young's scaling relation appears to hold quite well for telescope apertures up to 4-m, and for quite different sites (Kjeldsen & Frandsen 1991; Gilliland & Brown 1992; Gilliland et al. 1993). However recent studies by Kornilov et al. (2012) and Osborn et. al (2015) showed that this equation tends to underestimate the median scintillation noise at several major observatories around the world. Osborn et. al. (2015) presented a modified form of Young's approximation (equation 1) that uses empirical correction coefficients to give more reliable estimates of the scintillation noise at a range of astronomical sites:

$$\sigma_Y^2 = 10 \times 10^{-6} C_Y^2 D^{-4/3} t^{-1} (\cos \gamma)^{-3} \exp(-2h_{\text{obs}}/H), \quad (1)$$

where C_Y is the empirical coefficient, D is the diameter of the telescope, t is the exposure time of the observation, γ is the zenith distance, h_{obs} is the altitude of the observatory and H the scale height of the atmospheric turbulence, which is generally accepted to be approximately 8000-m. All parameters are in standard SI units. The empirical coefficients C_Y for the major observatories around the world are listed by Osborn et al. (2015).

The theoretical values of scintillation noise for Sutherland and Nainital were estimated using equation 1. The scintillation noise in terms of amplitude was obtained by taking the square root of σ_Y . However, in order to compare the two sites having different telescope diameters, we have to scale the theoretical values. Therefore, the theoretical scintillation noise for SAAO (50-cm telescope) was scaled to the aperture of the ARIES telescope (104-cm) using the same relation. The input parameters used to estimate the theoretical scintillation noise are : height (ARIES: 1958-m, SAAO : 1798-m), $\sec(Z)$ (airmass) : 1, C_Y : 1.5, integration time : 10-sec. The estimated scintillation values of ARIES (D:104-cm) and SAAO (D:50-cm) are 0.0338 mmag and 0.0433 mmag, respectively. The scaled value of the scintillation noise for SAAO (scaled to 104-cm) is 0.0340 mmag. Fig. 1 shows the theoretical noise levels for the ARIES and SAAO sites (both scaled and unscaled).

Since the observations in the Nainital-Cape survey were carried out over many nights, and in a variety of atmospheric conditions, the noise levels in the Fourier spectra of the individual light curves are expected to be higher than the theoretical scintillation values for each site, and they are also not expected to be white noise. In order to estimate the observational values of the noise in our amplitude spectra as a function of frequency, we first transformed the time-series data of stars observed from ARIES during 2006-2009 and from SAAO during 2006-2007 into their individual periodograms. We then combined all the periodograms from each site into a single pseudo-periodogram and fitted an acspline function to obtain the average estimated noise profile as a function of frequency. These observational noise curves are shown in Fig. 1 in solid blue for ARIES and dot-dashed red for SAAO. These noise profiles provide a useful first check of the significance of possible oscillation frequencies identified in the Fourier spectra in Fig. 3 of this paper.

More than half of the known roAp stars were discovered photometrically from SAAO. One of the basic reasons behind this is that the Sutherland site has stable and good sky transparency, allowing a closer match to scintillation noise than at many other observing sites used in other roAp surveys. However, in the last

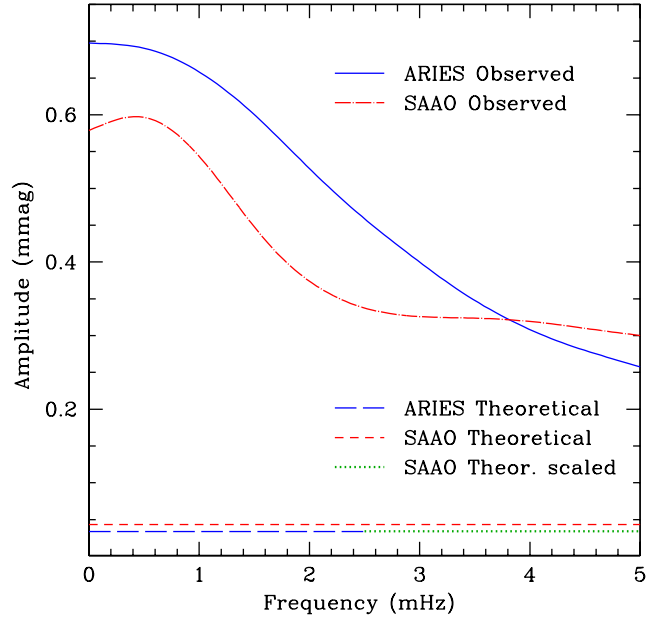


Fig. 1. The noise characteristics for the ARIES site at Nainital and the SAAO Sutherland site. The acspline-fitted curve of ARIES and SAAO amplitude spectra are shown in solid blue and dot-dashed red curve, respectively. The theoretical scintillation noise levels of ARIES and SAAO are shown by blue long-dashed and red small-dashed horizontal lines, respectively, and the scintillation noise level of SAAO (scaled to 104cm diameter) is also shown in green dotted horizontal line.

ten years that we have been running the Nainital-Cape Survey, we have noticed a gradual increase in sky brightness and atmospheric noise owing to enhanced human activities around the ARIES and Sutherland observatories. It can be inferred from the scaling relation (eqn. 1) that the combined atmospheric noise can be minimized by installing bigger telescopes at a good observing site where one can find stable photometric sky conditions (Young 1967). A new 1.3-m optical telescope is now operational at a new astronomical site of ARIES observatory known as Devasthal (longitude: 79°40'57" E, latitude : 29°22'26" N, altitude : 2420-m). In addition, a new 3.6-m telescope has been recently installed at the Devasthal site and is likely to be operational by 2016. The theoretical scintillation noise estimated for this telescope is 0.0217 mmag making the telescope very efficient for detecting tiny amplitude variations. The 0.5-m telescope of SAAO is also soon to be replaced with a 1.0-m robotic telescope. These up-coming observing facilities equipped with modern state-of-the-art instruments at ARIES and SAAO will be the next step to boost the Nainital-Cape survey and other projects aimed at the detection of sub-mmag light variations.

5. New Null Results from the Nainital-Cape Survey

In this paper we report the non-detections of pulsation in 108 CP stars. The first and second panels of Fig. 3 depict the light curves of the candidate stars observed from ARIES and SAAO. The pre-whitened frequency spectra of the respective time-series are plotted in the third and fourth columns. The name of the star, duration of observations in hours and the heliocentric Julian dates are marked in each panel.

Here it is worth recalling that roAp stars show amplitude modulation due to rotation and beating between multiple pulsation frequencies. Therefore, the non-detection of light variations may be due to fact that the observations are acquired at a time when the pulsations are below the detection limit of the survey. For example, Joshi et al. (2006) classified HD 25515 as a null result and then subsequently, after further observations, classified it as a δ Scuti type pulsating variable (Joshi et al. 2009). Hence, a null-detection of pulsations does not mean that the star is non-variable, but rather that its light output was not detected to vary during the particular interval of the observations. This demonstrates the necessity for repeated observations of the candidate stars. These null results are also an important contribution toward understanding the distinction between pulsating and non-pulsating CP stars that are otherwise similar in all other observational respects (Murphy et al. 2015). As mentioned above, a by-product of these null results is an observational characterisation of a particular observing site for data acquired on many nights over a wide range of observing conditions.

6. Comparison of Known roAp Stars with the Null Results

At the time the Nainital-Cape survey began, only 23 roAp stars were known. Therefore, our knowledge of the extent of the roAp phenomenon at that time was used to define the target selection and observing strategy. Since then, the number of known roAp stars has more than doubled, and currently stands at 61 confirmed members of this class. The compilation of the various physical parameters of the known roAp stars are important to study the roAp and noAp (“non-roAp”) phenomena in Ap stars. Tables 1 and 2 list the astrophysical parameters of the known roAp stars extracted from the available sources in the literature. For each star Table 1 lists, respectively, the table entry number, the HD number of roAp star, their popular name, spectral type, Strömgren indices $b - y$, m_1 , c_1 , β , δm_1 , δc_1 , effective temperature T_{eff} , and the reference(s) from which the data were taken. Table 2 lists the table entry number, the HD or HR catalogue number and other name(s) of the roAp star, the visual magnitude m_v , parallax π , distance d , absolute magnitude M_v , luminosity parameter $\log(\frac{L}{L_\odot})$, pulsational period corresponding to the highest amplitude, the frequency separation $\Delta\mu$, maximum photometric amplitude variation A_{max} , maximum radial velocity variation RV_{max} , rotational period P_{rot} , surface gravity $\log g$, mass M_\star , radius R_\star , mean longitudinal magnetic field and the projected rotational velocity $v \sin i$. Where no data is available in the data archives or in the literature for a given parameter, this is denoted with a “-” symbol in the relevant column. It is instructive to compare the coverage of the Nainital-Cape survey with the currently established extent of the roAp phenomenon. Therefore, the catalogue of the basic parameters of the known roAp stars can be used for the statistical analysis of roAp and noAp phenomena in Ap stars located in the same part of the H-R diagram.

7. Evolutionary States of the Studied Samples

To establish the evolutionary status of the sample null result stars, we first established their luminosities and effective temperatures, which then allowed us to compare them with the known roAp stars. The absolute magnitudes and luminosities of the candidate stars observed in the Nainital-Cape survey were determined based on the data taken from the Hipparcos catalogue

(van Leeuwen 2007). The photometric T_{eff} is calculated from the Strömgren β indices using the grids of Moon & Dworetzky (1985) that give a typical error of about 200 K. The various astrophysical parameters of the stars observed in the Nainital-Cape survey are listed in Table 3. These parameters are either taken from the Simbad database or calculated using the standard relations (Cox 1999). For each star, this Table lists the HD number, right ascension α_{2000} , declination δ_{2000} , visual magnitude m_v , spectral type, parallax π , Strömgren indices $b - y$, m_1 , c_1 , β , δm_1 , δc_1 , effective temperature T_{eff} , luminosity parameter $\log(\frac{L}{L_\odot})$, duration of the observations Δt , heliocentric Julian dates (HJD:2450000+) and year of observations (2000+) when the star was observed. The Strömgren indices δm_1 and δc_1 are calculated using the calibration of Crawford (1975, 1979).

The absolute magnitude M_v in the V-band was determined using the standard relation (Cox 1999),

$$M_v = m_v + 5 + 5 \log \pi - A_v, \quad (2)$$

where π is trigonometric parallax measured in arcsec, the interstellar extinction in the V-band is $A_v = R_v E(B-V) = 3.1 E(B-V)$. The reddening parameter $E(B-V)$ is obtained by taking the difference of the observed colour (taken from the Simbad data base) and intrinsic colour (estimated from Cox (1999)).

The stellar luminosity was calculated using the relation

$$\log \frac{L}{L_\odot} = -\frac{M_v + BC - M_{bol,\odot}}{2.5}, \quad (3)$$

where we adopted the solar bolometric magnitude $M_{bol,\odot} = 4.74$ mag (Cox 1999), and used the standard bolometric correction BC from Flower (1996). Taking into account all contributions to the M_v and $\frac{L}{L_\odot}$ error budgets, we find a typical uncertainty of 20-25% for both parameters.

The null objects displayed in Fig. 2 include all the objects from paper I,II,III and IV (this paper) of the Nainital-Cape survey. The positions of known roAp stars and the newly discovered δ -Scuti type variables in our survey are also shown. The evolutionary tracks for stellar masses ranging from 1.5 to 3.0 M_\odot (Christensen-Dalsgaard 1993) are over-plotted. The position of the blue (left) and red (right) edges of the instability strip are shown by two oblique lines (Turcotte et al. 2000). Fig. 2 clearly shows that most of the sample stars are located within the instability strip. For reasons given above, we may expect that some of the stars listed as null results in this paper may well turn out to be variables in near future. However, with each subsequent non-detection of pulsations, the constraint on non-variability will be strengthened and they will be established as “noAp” stars, thus helping to shed light on the other observational characteristics that will allow us to distinguish between pulsating and constant CP stars, which is one of the long-term goals of the Nainital-Cape survey.

8. Ground Based Surveys for Pulsation in Chemically Peculiar stars

In the past, several surveys have been conducted around the globe to search for roAp stars with different instrumental setups in both the northern and southern hemisphere independently. Such surveys required much telescope time, hence the photometric surveys were performed on 1-m class telescopes, on which it was possible to secure ample telescope time. Spectroscopic surveys became more popular in recent years due to improved

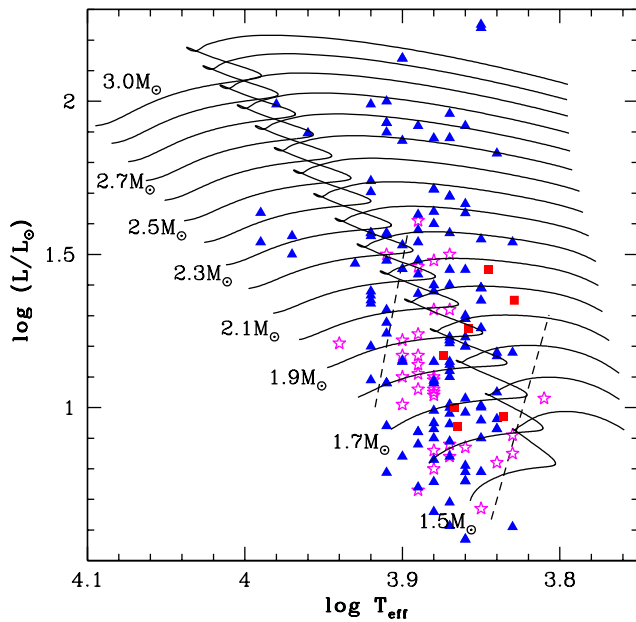


Fig. 2. The positions of the null results (filled triangle) and δ -Scuti type variables discovered under the Nainital-Cape survey (filled square). For comparison, positions of known roAp stars are also shown (open star). The solid lines show theoretical evolutionary tracks from the ZAMS (Christensen-Dalsgaard 1993). The dashed lines indicate the red and blue edges of the instability strip.

sensitivity of the high-resolution spectroscopic instruments used to search for low-amplitude oscillations in roAp candidates. The major drawback of this technique remains the small amount of observing time available on large telescopes. In this section, we provide a short description of the various surveys conducted for pulsation in CP stars.

8.1. Cape Survey

Following the discovery of first roAp star HD 101065 in 1978, only 14 stars were known prior to 1990. A systematic survey for roAp stars in the southern hemisphere was initiated by Don Kurtz and Peter Martinez at SAAO with two objectives: the first was to increase the number of members of this class and the second was to study the relationship between the roAp stars and the other pulsating stars located at the same region of the H-R diagram. The observations for this survey were acquired with the photoelectric photometers attached to the 0.5-m and 1.0-m telescopes at Sutherland. Under the Cape-survey 134 Southern Ap SrCrEu stars were checked for the pulsational variability and 12 new roAp stars were discovered (Martinez et al. 1991, Martinez & Kurtz 1994a, 1994b).

8.2. Nainital-Cape Survey

The detection of the small amplitude light variations needs a lot of observational expertise. As mentioned above most of the roAp stars known prior to 2000 were discovered under the Cape survey, where the SAAO astronomers gained a lot of observational experience. However, this meant that most of the known roAp stars were southern objects. The Nainital-Cape survey was initiated in 1999 as a collaboration between South African and

Indian astronomers to increase the number of known roAp stars in the northern sky. This survey was started in 1999 and lasted for ten years making it the most extensive survey for pulsation in CP stars, where a total of 337 Ap and Am stars were monitored. Although only one new roAp star, HD 12098, was discovered, in this survey, it revealed milli-magnitude level light variations with periods similar to those of the δ -Scuti stars in seven Am stars. This survey is thus unique in a sense that both the Ap and Am stars were included in the samples, hence there were plenty of chances to discover pulsations in CP1 and CP2 stars. The null results of this survey have been published in Martinez et al. (2001), Joshi et al. (2006, 2009) as well as in the present paper. The archive of well-established null results is useful to delineate the extent of the roAp phenomenon and also to shed light on the distinction between roAp and noAp stars.

8.3. Lowell-Wisconsin Survey

Between 1985 to 1991, Nelson & Kreidl (1993) conducted a survey of pulsation in 120 northern Ap stars of spectral range B8–F4. Though these authors did not report the discovery of any new roAp stars from their survey, their main finding was the absence of pulsation in the spectral range B8–A5, indicating that roAp-like oscillations are likely to be confined to the cooler peculiar stars.

8.4. The Hvar Survey

A photometric survey was initiated in 2011 to search for new northern roAp stars at the Hvar observatory (Paunzen et al. 2012, 2015). For this survey, a CCD based photometer attached to the 1.0-m Austrian-Croatian telescope was used for the observations of candidate stars. Under this survey, 80 candidate roAp stars were examined for a total duration of 100 hours. Differential CCD photometry was performed to detect the light variations in the sample Ap stars. The authors have not reported any positive detections and have presented the frequency spectra and the basic parameters of the null results they observed.

8.5. Other Minor Photometric Surveys

In addition to the above surveys, a number of smaller photometric surveys have also been conducted in the northern and southern hemisphere independently by Dorokhova & Dorokhov (1998), Kurtz (1982), Matthews et al. (1988), Heller & Kramer (1990), Schutt (1991), Belmonte (1989), Hildebrandt (1992), and Handler & Paunzen (1999). Though these surveys are small in terms of sample size and number of newly discovered roAp stars, they have helped to define candidate selection criteria for other roAp surveys.

8.6. Spectroscopic Surveys

Spectroscopy of high spectral and temporal resolution using large telescopes allows the detailed study of line profile variations (Hatzes & Mkrtichian 2005). After the discovery of significant RV pulsational variations in some known roAp stars (Kanaan & Hatzes 1998), candidate roAp stars have been monitored with time-resolved high-resolution spectroscopic observations by several observers in the last ten years. These observations have revealed that the highest RV amplitudes are observed in the spectral lines of the rare-earth elements, while spectral lines of the other elements show weak or undetectable os-

cillations. Using spectroscopic techniques, about 15 roAp stars have been discovered (Kochukhov 2006; Kochukhov et al. 2008; 2009; Kochukhov et al. 2013; Alentive et al. 2012; Elkin et al. 2005a; 2005b; Kurtz et al. 2006).

9. Conclusions

In this paper, we have presented the light curves and frequency spectra of the 108 candidate stars observed in the Nainital-Cape survey. Analyses of the photometry acquired at Sutherland and Nainital indicate that we have achieved a detection level of about 0.6 mmag in the frequency range 1-5 mHz in the Nainital-Cape survey. Using the standard relations and data extracted from the literature we have presented the various astrophysical parameters of the null results. We have also compiled the basic physical parameters of the known roAp stars. On comparing the positions of the known roAp stars to the observed sample stars in the H-R diagram, we infer that the boundary of the roAp phenomenon extends beyond the cool edge of the classical instability strip.

Acknowledgments

This work was carried out under the Indo-South Africa Science and Technology Cooperation INT/SAFR/P-3(3)2009) and NRF grant UID69828 funded by Departments of Science and Technology of the Indian and South African Governments. SC acknowledges support under the Indo-Russian grant INT/RFBR/P-118 through which he received a stipend to perform this work. SC also thanks the ARIES academic committee for their help and support. We acknowledge use of SIMBAD, NASA's ADS and ESA's Hipparcos database.

References

- Abt, H. A., & Golson, J. C. 1962, *ApJ*, 136, 35
- Abt, H. A., & Snowden, M. S. 1973, *ApJS*, 25, 137
- Alentiev, D., Kochukhov, O., Ryabchikova, T., et al. 2012, *MNRAS*, 421, L82
- Ashoka, B. N., Kumar, Babu, V. C., et al. 2001, *JA&A*, 22, 131
- Babel, J. 1992, *A&A*, 258, 449
- Balmforth, N. J., Cunha, M. S., Dolez, N., et al. 2001, *MNRAS*, 323, 362
- Balona, L. A., & Laney, C. D. 2003, *MNRAS*, 344, 242
- Balona, L. A., Cunha, M. S., Gruberbauer, M., et al. 2011, *MNRAS*, 413, 2651
- Balona, L. A., Catanzaro, G., Crause, L., Cunha, M., et al. 2013, *MNRAS*, 432, 2808
- Balona, L. A., Catanzaro, G., Abedigamba, O. P., et al. 2015, *MNRAS*, 448, 1378
- Belmonte, J. A. 1989, Ph.D. Thesis, Universidad de La Laguna, Tenerife
- Bychkov V. D., Bychkova L. V. & Madej J. 2003, *A&A*, 407, 631
- Catanzaro, G., & Ripepi, V. 2014, *MNRAS*, 441, 1669
- Christensen-Dalsgaard J., 1993, Baglin, A., Weiss, W. W., eds, *ASP Conf. Ser. Vol. 40, Proc. IAU Coll. 137, Inside the stars*. ASP, San Francisco, 483
- Cox, A. N. 1999, *Allen's Astrophysical Quantities*
- Crawford, D. L. 1975, *AJ*, 80, 955
- Crawford, D. L. 1979, *AJ*, 84, 1858
- Cunha, M. S., & Gough, D. 2001, *ESASP*, 464, 419
- Deeming, T. J. 1975, *Ap&SS*, 36, 137
- Dorokhova, T. N., & Dorokhov, N. I. 1998, *Contrib. Astron. Obser. Skalnate Pleso*, 27, 338
- Elkin, V. G., Riley, J. D., Cunha, M. S., Kurtz, D. W., Mathys, G. 2005a, *MNRAS*, 358, 665
- Elkin, V. G., Kurtz, D. W., & Mathys, G. 2005b, *MNRAS*, 364, 864
- Elkin, V. G., Kurtz, D. W., Mathys, G., Freyhammer, L. M. 2010, *MNRAS*, 402, 1883
- Elkin, V. G., Kurtz, D. W., Worters, H. L., et al. 2011, *MNRAS*, 411, 978
- Flower, P. J. 1996, *ApJ*, 469, 355
- Gilliland, R. L., & Brown, T. M. 1992, *PASP*, 104, 582
- Gilliland, R. L., Brown, T. M., Kjeldsen, H., et al. 1993, *AJ*, 106, 2441
- Girish, V., Seetha, S., Martinez, P., et al. 2001, *A&A*, 380, 142
- González, J. F., Hubrig, S., Kurtz, D. W., Elkin, V. G., Savanov, I. 2008, *MNRAS*, 384, 1140
- Handler, G., & Paunzen, E. 1999, *A&AS*, 135, 57
- Handler, G., Weiss, W. W., Paunzen, E., et al. 2002, *MNRAS*, 330, 153
- Handler, G., Weiss, W. W., Shobbrook, R., et al. 2006, *MNRAS*, 366, 257
- Hatzes, A. P., & Mkrichian, D. E. 2004, *MNRAS*, 351, 2
- Hatzes, A. P., & Mkrichian, D. E. 2005, *A&A*, 430, 279
- Heller, C. H., & Kramer, K. S. 1990, *MNRAS*, 244, 372
- Hildebrandt, G. 1992, *Astron. Nachr.*, 313, 233
- Holdsworth, D. L., Smalley, B., Gillon, M., et al. 2014a, *MNRAS*, 439, 2078
- Holdsworth D. L., Smalley, B., Kurtz, D. W., et al. 2014b, *MNRAS*, 443, 2049
- Holdsworth, D. L. 2015, PhD Thesis, Keele University, UK
- Hou, Wen, Luo, ALi, Yang, Haifeng, et al. 2015, *MNRAS*, 449, 1401
- Hubrig, S., Kurtz, D. W., Schöller M., et al. 2012, *ASPC*, 462, 318
- Joshi, S., Girish, V., Sagar, R., et al. 2003, *MNRAS*, 344, 431
- Joshi, S., Mary, D. L., Martinez, P., et al. 2006, *A&A*, 455, 303
- Joshi, S., Mary, D. L., Chakradhari, N. K., Tiwari, S. K., Billaud, C. 2009, *A&A*, 507, 1763
- Joshi, S., & Joshi, Y. C. 2015, *JA&A*, 36, 33
- Kanaan, A., & Hatzes, A. P. 1998, *ApJ*, 503, 848
- Kjeldsen, H., & Frandsen, S. 1991, *A&AS*, 87, 119
- Koch, D. G., Borucki, W. J., Basri, G. et al. 2010, *ApJ*, 713, L79
- Kochukhov, O. 2006, *A&A*, 446, 1051
- Kochukhov, O., & Ryabchikova, T. 2001, *A&A*, 374, 615
- Kochukhov, O., Ryabchikova, T., Bagnulo, S., Lo Curto, G. 2008, *A&A*, 479, L29
- Kochukhov, O., Bagnulo, S., Lo Curto, G., Ryabchikova, T. 2009, *A&A*, 493, L45
- Kochukhov, O., Alentiev, D., Ryabchikova, T., et al. 2013, *MNRAS*, 431, 2808
- Kornilov, V., Sarazin, M., Tokovinin, A., Travouillon, T., Voziakova, O. 2012, *A&A*, 546, A41
- Kreidl, T. J., & Kurtz, D. W. 1986, *MNRAS*, 220, 313
- Kreidl, T. J., Kurtz, D. W., Bus, S. J., et al. 1991, *MNRAS*, 250, 477
- Kurtz, D. W. 1978, *IBVS*, 1436, 1
- Kurtz, D. W. 1982, *MNRAS*, 200, 807
- Kurtz, D. W. 1985, *MNRAS*, 213, 773
- Kurtz, D. W. 1991, *MNRAS*, 249, 468
- Kurtz, D. W., & Martinez, P. 1987, *MNRAS*, 226, 187
- Kurtz, D. W., & Martinez, P. 1994, *IBVS*, 4013, 1
- Kurtz, D. W., Sullivan, D. J., Martinez, P., Tripe, P. 1994a, *MNRAS*, 270, 674
- Kurtz, D. W., Martinez, P., & Tripe, P. 1994b, *MNRAS*, 271, 421
- Kurtz, D. W., & Martinez, P. 1995, *IBVS*, 4209, 1
- Kurtz, D. W., Martinez, P., Koen, C., Sullivan, D. J. 1996, *MNRAS*, 281, 883
- Kurtz, D. W., van Wyk, F., Roberts, G., et al. 1997a, *MNRAS*, 287, 69
- Kurtz, D. W., Martinez P., Tripe, P., Hanbury, A. G. 1997b, *MNRAS*, 289, 645
- Kurtz, D. W., Elkin, V. G., & Mathys, G. 2003, *MNRAS*, 343, L5
- Kurtz, D. W., Elkin, V. G., & Mathys, G. 2005a, *MNRAS*, 358, L6
- Kurtz, D. W., Elkin, V., Savanov, I., et al. 2005b, *MNRAS*, 358, 651
- Kurtz, D. W., Elkin, V. G., & Mathys, G. 2006, *MNRAS*, 370, 1274
- Kurtz, D. W., Cunha, M. S., Saio, H., et al. 2011, *MNRAS*, 414, 2550
- Martinez, P. & Kurtz, D. W. 1990, *MNRAS*, 242, 636
- Martinez, P., Kurtz, D. W., & Heller, C. H. 1990, *MNRAS*, 246, 699
- Martinez, P., Kurtz, D. W., & Kauffmann, G. M. 1991, *MNRAS*, 250, 666
- Martinez, P., Kurtz, D. W., & Meitjes, P. J. 1993, *MNRAS*, 260, 9
- Martinez, P., & Kurtz, D. W. 1994a, *MNRAS*, 271, 118
- Martinez, P., & Kurtz, D. W. 1994b, *MNRAS*, 271, 129
- Martinez, P., Weiss, W. W., Nelson, M. J., et al. 1996, *MNRAS*, 282, 243
- Martinez, P., Meintjes, P., Ratcliff, S. J., Engelbrecht, C. 1998, *A&A*, 334, 606
- Martinez, P., Kurtz, D. W., Ashoka, B. N., et al. 2001, *A&A*, 371, 1048
- Matthews, J. M., Wehlau, W. H., & Kurtz, D. W. 1987, *ApJ*, 313, 782
- Matthews, J. M., Kreidl, T. J., & Wehlau, W. H. 1988, *PASP*, 100, 255
- Medupe, R., Kurtz, D. W., Elkin, V. G., Mguda, Z., Mathys, G. 2015, *MNRAS*, 446, 1347
- Michaud, G. 1970, *ApJ*, 160, 641
- Michaud, G., Charland, Y., & Megessier, C. 1981, *A&A*, 103, 244
- Mkrichian, D. E., Hatzes, A. P., & Kanaan, A. 2003, *MNRAS*, 345, 781
- Mkrichian, D. E., & Hatzes, A. P. 2005a, *A&A*, 430, 263
- Mkrichian, D. E., & Hatzes, A. P. 2005b, *JApA*, 26, 185
- Moon, T., & Dworetzky, M. M. 1985, *MNRAS*, 217, 305
- Murphy, S. J., Bedding, T. R., Niemczura, E., Kurtz, D. W., Smalley, B. 2015, *MNRAS*, 447, 3948
- Nelson, M. J., & Kreidl, T. J. 1993, *AJ*, 105, 1903
- Osborn, J., Föhning, D., Dhillon, V. S., Wilson, R. W. 2015, *MNRAS*, 452, 1707
- Paunzen, E., Netopil, M., Rode-Paunzen, M., et al. 2012, *A&A*, 542A, 89
- Paunzen, E., Netopil, M., Rode-Paunzen, M., et al. 2015, *A&A*, 575A, 24
- Preston, G. W. 1974, *ARA&A*, 12, 257
- Renson, P., & Manfroid, J. 2009, *A&A*, 498, 96
- Renson P., Gerbaldi M., Catalano F. A., 1991, *A&AS*, 89, 429
- Richer, J., Michaud, G., & Turcotte, S. 2000, *ApJ*, 529, 338

- Ryabchikova, T., Nesvacil, N., Weiss, W. W., Kochukhov, O., Stütz, Ch. 2004, A&A, 423, 705
- Schneider, H., Kreidl, T. J., & Weiss, W. W. 1992, A&A, 257, 130
- Schutt, R. 1991, AJ, 101, 2177
- Schwarzenberg-Cherny, A., 1996, ApJ, 460, 107
- Smalley, B., Kurtz, D. W., Smith, A. M. S., et al. 2011, A&A, 535, 3
- Smalley, B., Niemczura, E., Murphy, S. J., et al. 2015, MNRAS, 452, 3334
- Turcotte, S., Richer, J., Michaud, G., Christensen-Dalsgaard, J. 2000, A&A, 360, 603
- van Leeuwen, F. 2007, A&A, 474, 653
- Young, A. T. 1967, AJ, 72, 747
- Young, A. T. 1974, ApJ, 189, 587

Table 1. The known roAp stars and their physical parameters.

S.N.	Star Name	Other Name	α_{2000}	δ_{2000}	Sp. Type	b-y mag	m_1 mag	c_1 mag	δm_1 mag	δc_1 mag	β mag	T_{eff} K	Ref.
1.		J0008	00 08 30	+04 28 18	A9p SrEu(Cr)	-	-	-	-	-	-	7300	1
2.	HD6532		01 05 56	-26 43 44	ApSrCrEu	0.082	0.233	0.870	-0.014	-0.051	2.882	7900	2
3.	HD9289		01 31 16	-11 07 08	ApSrEu	0.138	0.225	0.826	-0.018	-0.012	2.833	8000	3,4
4.	HD12098		02 00 40	+58 31 37	F0	0.191	0.328	0.517	-0.122	-0.279	2.796	7500	5
5.	HD12932		02 06 16	-19 07 26	ApSrEuCr	0.179	0.228	0.765	-0.024	-0.035	2.810	7620	6
6.	HD19918		03 00 37	-81 54 07	Ap SrEuCr	0.169	0.216	0.822	-0.010	-0.058	2.855	7800	4
7.	HD24355	J0353	03 53 23	25 38 33	A5p SrEu	-	-	-	-	-	-	8250	1
8.	HD24712	HR 1217	03 55 16	-12 05 57	ApSrEu(Cr)	0.191	0.211	0.626	-0.023	-0.074	2.744	7250	7,8,9
9.	HD42659		06 11 22	-15 47 35	ApSrCrEu	0.124	0.257	0.765	-0.050	-0.076	2.834	7500	4
10.	HD258048	J0629	06 29 57	+32 24 47	F4p EuCr(Sr)	-	-	-	-	-	-	6600	1
11.		J0651	06 51 42	-63 25 50	F0p SrEu(Cr)	-	-	-	-	-	-	7400	1
12.	HD60435		07 30 57	-57 59 28	ApSr(Eu)	0.136	0.240	0.833	-0.034	-0.047	2.855	7800	10
13.	HD69013		08 14 29	-15 46 32	A2SrEu	0.296	0.330	0.400	-0.137	-0.324	2.772	7600	11
14.	HD75445		08 48 43	-39 14 02	SrEu	0.159	0.218	0.729	-0.019	0.001	2.801	7650	12
15.		J0855	08 55 22	+32 42 36	A6p SrEu	-	-	-	-	-	-	7800	1
16.	HD80316		09 18 25	-20 22 16	ApSr(Eu)	0.118	0.324	0.599	-0.118	-0.283	2.856	7700	13
17.	HD83368	HR 3831	09 36 25	-48 45 04	A8pSrEuCr	0.159	0.230	0.766	-0.024	-0.062	2.825	7650	7,14,15
18.	HD84041		09 41 34	-29 22 25	ApSrEuCr	0.177	0.233	0.797	-0.026	-0.061	2.844	7500	4
19.	HD86181		09 54 53	-58 41 45	ApSr	0.172	0.205	0.757	0.001	-0.061	2.819	7900	16
20.	HD92499		10 40 08	-43 04 51	A2SrCrEu	0.179	0.301	0.615	-0.099	0.000	2.812	7500	17
21.	HD96237		11 05 34	-25 01 09	A4SrEuCr	0.233	0.261	0.704	-0.054	-0.122	2.824	7800	11
22.	HD97127	J1110	11 10 54	+17 03 48	F3p SrEu(Cr)	-	-	-	-	-	-	6300	1
23.	HD99563		11 27 17	-08 52 08	F0	0.171	0.206	0.745	-0.001	-0.090	2.830	7000	18,19,20
24.	HD101065	Przbylski's star	11 37 37	-46 43 00	Controversial	0.431	0.387	0.002	-0.204	-0.370	2.641	6800	7,21,22
25.	HD115226		13 18 00	-72 57 01	A3pSr	-	-	-	-	-	-	7600	23
26.	HD116114		13 21 46	-18 44 32	ApSrCrEu	0.172	0.226	0.843	-0.016	0.008	2.836	7600	24
27.	HD119027		13 41 20	-28 46 60	ApSrEu(Cr)	0.257	0.214	0.557	-0.034	-0.076	2.731	7050	25
28.		J1430	14 30 50	+31 47 55	A9p SrEu	-	-	-	-	-	-	7100	1
29.	HD122970		14 04 49	+05 24 51	F0	0.260	0.178	0.540	-0.005	-0.011	2.707	7000	26
30.	HD128898	α Cir	14 42 30	-64 58 30	ApSrEu(Cr)	0.152	0.195	0.760	0.012	-0.077	2.831	7500	7,27,28
31.	HD132205		15 00 04	-55 02 60	A2EuSrCr	-	-	-	-	-	-	7800	29
32.	HD134214		15 09 02	-13 59 59	ApSrEu(Cr)	0.216	0.223	0.620	-0.029	-0.108	2.774	7400	30
33.	HD137909	β CrB	15 27 50	+29 06 20	F0p	0.141	0.257	0.740	-0.056	0.002	2.839	7800	31
34.	HD137949	33 Lib	15 29 35	-17 26 27	ApSrEuCr	0.196	0.311	0.580	-0.105	-0.236	2.818	7700	32,33,34
35.	HD143487		16 01 44	-30 54 57	A3SrEuCr	0.311	0.262	0.393	-0.089	-0.169	2.706	7000	17
36.	HD148593		16 29 39	-14 35 06	A2 Sr	-	-	-	-	-	-	7850	29
37.		J1640	16 40 03	-07 37 30	A8p SrEu	-	-	-	-	-	-	7400	1
38.	HD150562		16 44 11	-48 39 18	A/F (pEu)	0.301	0.212	0.659	-0.015	-0.087	2.783	7500	4
39.	HD151860		16 52 59	-54 09 46	A2SrEu	0.327	0.221	0.538	-	-	-	7050	29

⁰ 1. Holdsworth et al. (2014a); 2. Kurtz et al. (1996); 3. Kurtz et al. (1994b); 4. Martinez & Kurtz (1994a); 5. Girish et al. (2001); 6. Schneider et al. (1992); 7. Kurtz (1982); 8. Kurtz et al. (2005b); 9. Mkrtichian & Hatzes (2005a); 10. Matthews et al. (1987); 11. Elkin et al. (2011); 12. Kochukhov et al. (2009); 13. Kurtz et al. (1997b); 14. Kochukhov (2006); 15. Kurtz et al. (1997a); 16. Kurtz & Martinez (1994); 17. Elkin et al. (2010); 18. Dorokhova & Dorokhov (1998); 19. Handler et al. (2006); 20. Elkin et al. (2005b); 21. Mkrtichian & Hatzes (2005b); 22. Martinez & Kurtz (1990); 23. Kochukhov et al. (2008); 24. Elkin et al. (2005a); 25. Martinez et al. (1993); 26. Handler et al. (2002); 27. Balona & Laney (2003); 28. Kurtz et al. (1994a); 29. Kochukhov et al. (2013); 30. Kreidl & Kurtz (1986); 31. Hatzes & Mkrtichian (2004); 32. Kurtz et al. (2005a); 33. Mkrtichian et al. (2003); 34. Kurtz (1991); 35. Kurtz et al. (2006); 36. Martinez et al. (1991); 37. Kurtz et al. (2003); 38. Kurtz & Martinez (1987); 39. Holdsworth et al. (2014b); 40. Hatzes & Mkrtichian (2005); 41. Heller & Kramer (1990); 42. Kurtz et al. (2011); 43. Balona et al. (2013); 44. Alentiev et al. (2012); 45. Holdsworth (2015); 46. Kurtz & Martinez (1995); 47. Balona et al. (2011); 48. Smalley et al. (2015); 49. Kochukhov & Ryabchikova (2001); 50. Martinez et al. (1996); 51. Martinez et al. (1990); 52. Martinez et al. (1998); 53. Kreidl et al. (1991); 54. Gonzalez et. al (2008).

Table 1. continued.

S.N.	Star Name	Other Name	α_{2000}	δ_{2000}	Sp. Type	b-y mag	m_1 mag	c_1 mag	δm_1 mag	δc_1 mag	β mag	T_{eff} K	Ref.
40.	HD154708		17 10 28	-58 00 17	Ap	0.277	0.256	0.464	-0.079	0.015	2.757	7200	35
41.	HD161459		17 48 30	+51 55 02	ApEuSrCr	0.245	0.246	0.679	-0.040	-0.141	2.820	7950	36
42.	HD166473		18 12 26	-37 45 09	ApSrEuCr	0.208	0.321	0.514	-0.118	-0.268	2.801	7700	37,38
43.		KIC 007582608	18 44 12	+43 17 51	Ap	-	-	-	-	-	-	8700	39
44.	HD176232	10 Aql	18 58 47	+13 54 24	F0pSrEu	0.150	0.208	0.829	-0.004	0.031	2.809	7400	40,41
45.		KIC 010195926	19 05 27	+47 15 48	Ap	-	-	-	-	-	-	7400	42
46.		KIC 008677585	19 06 28	+44 50 33	A5p	-	-	-	-	-	-	7600	43
47.	HD177765		19 07 10	-26 19 54	A5SrEuCr	0.248	0.261	0.731	-0.054	-0.110	2.834	8000	44
48.		J1921	19 21 29	+47 10 53	F3p SrEuCr	-	-	-	-	-	-	6200	45
49.	HD185256		19 39 20	-29 44 34	ApSr(EuCr)	0.277	0.185	0.615	-0.004	-0.039	2.738	7250	46
50.		J1940	19 40 08	-44 20 09	F2(p Cr)	-	-	-	-	-	-	6900	1
51.		KIC 010483436	19 46 29	+47 37 50	Ap	-	-	-	-	-	-	7388	47
52.	HD225914	KIC 004768731	19 48 26	+39 51 58	Ap	-	-	-	-	-	-	7726	48
53.	HD190290		20 13 56	-78 52 42	ApEuSr	0.289	0.293	0.466	-0.091	-0.306	2.796	7500	36
54.	HD193756		20 24 12	-51 43 25	ApSrCrEu	0.181	0.213	0.760	-0.008	-0.040	2.810	7500	36
55.	HD196470		20 38 10	-17 30 06	ApSrEu(Cr)	0.211	0.263	0.650	-0.059	-0.144	2.807	7850	36
56.	HD201601	γ Equ	21 10 20	+10 07 54	F0p	0.147	0.238	0.760	-0.032	-0.058	2.819	7600	49,50
57.	HD203932		21 26 04	-29 55 48	ApSrEu	0.175	0.196	0.742	0.004	-0.020	2.791	7200	51
58.	HD213637		22 33 12	-20 02 22	A(pEuSrCr)	0.298	0.206	0.411	-0.035	-0.031	2.670	6400	52
59.	HD217522		23 01 47	-44 50 27	Ap(Si)Cr	0.289	0.227	0.484	-0.056	-0.015	2.691	7100	53
60.	HD218495		23 09 28	-63 39 12	A2pEuSr	0.114	0.252	0.812	-0.049	-0.098	2.870	8000	36
61.	HD218994		23 13 16	-60 35 03	A3Sr	0.154	0.196	0.826	0.008	0.032	2.807	7600	54

Table 2. Additional parameters for the known roAp stars.

S.N.	Star Name	m_v mag	π mas	d pc	M_V mag	$\log(L_\star/L_\odot)$	P_{pul} min	$\Delta\mu$ μHz	A_{max} mmag	RV_{max} kms^{-1}	P_{rot} days	$\log g$ dex	M_\star M_\odot	R_\star R_\odot	Mag. Field kG	vsini kms^{-1}
1.	J0008	10.16	-	-	-	-	9.58	-	0.76	-	-	-	-	-	-	-
2.	HD6532	8.40	6.14	162.87	2.20	1.22	7.10	47	5.00	1.15	1.94	4.30	-	-	0.22	30
3.	HD9289	9.38	-	-	2.42	-	10.52	-	3.50	0.85	8.55	4.15	-	-	0.65	10.5
4.	HD12098	8.07	-	-	-	-	7.61	-	3.00	-	5.46	4.20	1.70	1.70	1.46	10
5.	HD12932	10.25	-	-	2.55	-	11.61	-	4.00	1.40	3.53	4.15	-	-	1.20	2.50
6.	HD19918	9.34	4.07	245.70	2.34	1.06	11.04	-	2.00	1.30	-	4.34	-	-	1.60	3.00
7.	HD24355	9.65	-	-	-	-	6.42	-	1.38	-	13.95	-	-	-	-	-
8.	HD24712	6.00	20.32	49.21	2.32	0.87	6.13	68	10.00	0.25	12.46	4.30	1.55	1.77	3.10	5.60
9.	HD42659	6.76	7.60	131.58	2.38	1.48	9.70	52	0.80	0.70	-	4.40	2.10	-	0.39	19.00
10.	HD258048	10.52	-	-	-	-	8.49	-	1.49	-	-	-	-	-	-	-
11.	J0651	11.51	-	-	-	-	10.88	-	0.79	-	-	-	-	-	-	-
12.	HD60435	8.89	4.41	226.76	1.54	1.14	11.90	52	16.00	1.90	7.68	4.40	1.82	-	0.30	10.8
13.	HD69013	9.56	-	-	-	-	11.22	-	-	0.20	-	4.50	-	-	2.90	6.0
14.	HD75445	7.12	9.30	108.34	1.96	1.17	9.00	-	-	0.29	2.08	4.32	1.81	-	2.98	2
15.	J0855	10.80	-	-	-	-	7.30	-	1.40	-	3.09	-	-	-	-	-
16.	HD80316	7.78	7.25	137.93	2.26	1.11	7.40	-	2.00	0.32	2.08	4.58	1.70	1.53	0.18	32.0
17.	HD83368	6.17	14.16	70.62	2.47	1.09	11.60	-	10.00	3.33	2.85	4.20	1.76	2.00	0.50	33.0
18.	HD84041	9.33	-	-	2.38	-	15	60	6.00	0.50	3.69	4.30	-	-	0.48	25.0
19.	HD86181	9.32	3.49	286.53	2.49	1.01	6.20	-	4.60	-	-	-	-	-	0.40	-
20.	HD92499	8.89	3.54	282.48	1.63	1.05	10.40	-	-	0.066	-	4.00	1.68	-	8.15	3.3
21.	HD96237	9.43	1.53	653.59	-	1.61	13.89	-	-	0.10	-	4.30	-	-	2.90	6
22.	HD97127	9.43	-	-	-	-	13.51	-	0.66	-	-	-	-	-	-	-
23.	HD99563	8.67	3.92	255.10	1.90	1.10	10.70	-	10.00	4.9	2.91	4.20	2.03	1.90	0.57	28.0
24.	HD101065	7.99	8.93	111.98	2.09	0.91	12.16	68	13.00	1.03	3.94	4.20	1.52	1.98	2.30	4.0
25.	HD115226	8.51	6.80	147.06	2.67	0.86	10.86	-	-	1.24	3.30	4.00	1.60	-	0.75	27
26.	HD116114	7.02	7.71	129.70	1.35	1.32	21.30	-	-	0.65	-	4.10	2.07	-	0.50	2.2
27.	HD119027	10.02	-	-	3.04	0.67	8.63	52	2.00	0.148	-	4.40	-	-	3.10	4.0
28.	J1430	11.56	-	-	-	-	6.11	-	1.06	-	-	-	-	-	-	-
29.	HD122970	8.33	8.67	115.34	2.94	0.82	11.18	68	2.00	1.05	3.88	4.20	1.50	1.80	0.22	4.2
30.	HD128898	3.20	60.35	16.57	1.90	1.04	6.82	50	5.00	0.80	4.48	4.20	1.70	1.90	1.50	13.5
31.	HD132205	8.72	-	-	-	-	7.14	-	-	0.097	-	4.40	-	-	5.20	9.50
32.	HD134214	7.46	9.74	102.67	2.60	0.88	5.69	-	7.00	0.72	248	4.05	1.60	1.80	2.70	2.6
33.	HD137909	3.68	29.17	34.28	1.17	1.46	16.20	-	-	0.04	18.49	4.40	1.60	1.45	5.30	3.5
34.	HD137949	6.67	11.28	88.65	1.88	1.17	8.27	40	3.00	0.33	-	4.30	1.78	2.60	4.70	3.0
35.	HD143487	9.42	-	-	-	-	9.63	-	-	0.047	-	5.00	-	-	4.70	1.5
36.	HD148593	9.13	-	-	-	-	10.69	-	-	-	-	4.40	-	-	3.00	5.00
37.	J1640	12.67	-	-	-	-	9.48	-	3.52	-	3.67	-	-	-	-	-
38.	HD150562	9.82	-	-	2.68	-	10.80	50	0.80	0.14	-	4.40	-	-	5.00	1.5
39.	HD151860	9.01	-	-	-	-	12.30	-	-	-	0.083	4.50	-	-	2.50	4.5
40.	HD154708	8.76	6.75	148.15	2.39	0.73	8.00	-	-	0.09	5.37	4.11	1.50	1.70	24.50	4.0
41.	HD161459	10.33	-	-	2.47	-	12.00	-	1.30	-	-	4.38	-	-	1.76	-
42.	HD166473	7.92	-	-	2.52	1.24	8.80	68	2.00	0.10	-	4.47	1.80	-	8.50	2.5
43.	KIC 007582608	11.25	-	-	-	1.21	7.90	-	1.45	-	20.45	4.30	2.37	1.77	3.05	-
44.	HD176232	5.89	12.76	78.37	2.55	1.32	11.60	51	0.60	0.54	-	4.10	2.00	2.50	1.40	2.7
45.	KIC010195926	10.66	-	-	-	1.50	17.14	55	0.078	171	5.68	3.60	1.70	3.60	5	21
46.	KIC008677585	10.19	-	-	-	0.80	10.28	37.2	0.033	-	4.30	3.90	1.80	2.50	3.20	4.2
47.	HD177765	9.15	-	-	-	1.50	23.6	-	-	0.148	-	3.80	2.20	-	3.60	2.5

Table 2. continued.

S.N.	Star Name	m_v mag	π mas	d pc	M_V mag	$\log(L_\star/L_\odot)$	P_{pul} min	$\Delta\mu$ μHz	A_{max} mmag	RV_{max} kms^{-1}	P_{rot} days	$\log g$ dex	M_\star M_\odot	R_\star R_\odot	Mag. Field kG	vsini kms^{-1}
48.	J1921	12.16	-	-	-	-	11.18	-	1.99	-	-	-	-	-	-	-
49.	HD185256	9.94	-	-	-	-	10.33	-	3.00	0.15	-	4.30	-	-	0.71	6.2
50.	J1940	13.02	-	-	-	-	8.16	-	4.16	-	9.58	-	-	-	-	-
51.	KIC 010483436	11.43	-	-	-	0.84	12.32	-	0.068	-	4.30	4.15	1.60	1.61	-	20
52.	KIC 004768731	9.17	-	-	-	-	23.4	-	0.062	-	-	-	-	-	-	-
53.	HD190290	9.91	-	-	2.49	-	7.34	40	2.00	0.50	4.03	4.54	-	-	3.23	16
54.	HD193756	9.20	-	-	2.55	-	13.00	-	0.90	0.74	-	4.29	-	-	0.19	17.0
55.	HD196470	9.72	-	-	2.52	-	10.80	-	0.70	-	-	4.37	-	-	1.48	-
56.	HD201601	4.68	27.55	36.30	2.49	1.10	12.40	30	3.00	0.58	-	4.20	1.74	2.16	3.80	2.5
57.	HD203932	8.82	-	-	2.65	-	5.94	66	2.00	0.33	-	4.30	-	-	0.267	4.7
58.	HD213637	9.61	-	-	-	1.03	11.50	-	1.50	0.36	<25	3.60	1.60	-	0.74	3.5
59.	HD217522	7.52	11.36	88.03	2.77	0.85	13.70	58	4.00	0.12	8.55	4.20	1.49	1.86	1.70	2.7
60.	HD218495	9.38	-	-	2.23	-	7.44	-	1.00	0.79	-	4.40	-	-	0.91	16.0
61.	HD218994	8.56	3.55	281.69	1.25	1.06	14.20	-	-	0.093	-	4.10	-	-	0.440	5.2

Table 3. CP stars observed for pulsation from ARIES and SAO and classified as null results in this survey. Their physical parameters are listed.

S.N.	Star HD	α_{2000}	δ_{2000}	m_v mag	Sp. Type	π mas	b-y mag	m_1 mag	c_1 mag	β mag	δm_1 mag	δc_1 mag	T_{eff} K	$\log(L/L_\odot)$	Δt hr	HJD	Year of Observation
1.	1169	00 16 05	+08 06 56	7.60	A5	8.83±0.69	0.187	0.240	0.716	2.772	-0.047	-0.008	7455	1.18	0.45	4365	07
															1.07	4366	07
2.	1486	00 19 18	+59 08 20	7.28	B9V	6.32±0.83	-	-	-	-	-	-	-	-	2.78	4071	06
															2.41	4367	07
															1.91	4375	07
															3.73	4376	07
															1.42	4400	07
															2.18	4401	07
															3.22	4402	07
															2.84	4428	07
															2.09	4429	07
3.	2837	00 32 09	+43 42 42	9.16	A0p	2.75±1.08	-	-	-	-	-	-	-	-	1.42	4459	07
4.	3321	00 36 22	+33 38 39	8.42	A3	6.34±0.90	-	-	-	-	-	-	-	-	2.07	4397	07
5.	6757	01 08 53	+45 12 27	7.70	A0Vp	3.35±0.91	-	-	-	-	-	-	-	-	1.35	4427	07
															1.01	4431	07
6.	7676	01 16 07	-34 08 56	8.37	A5p	3.50±0.74	0.085	0.280	0.715	2.830	-0.073	-0.120	8008	1.47	1.95	4097	06
7.	8441	01 24 19	+43 08 32	6.67	A2p	4.88±0.59	0.022	0.141	1.145	2.833	0.066	0.306	9617	1.97	2.30	4751	08
8.	8783	01 24 00	-72 19 28	7.82	Ap	3.99±0.44	0.072	0.199	1.086	-	-	-	-	-	2.89	4077	06
9.	11090	01 46 35	-67 28 06	10.78	Ap	-	-	-	-	-	-	-	-	-	1.19	2127	01
															3.45	2128	01
10.	11948	01 58 51	+55 34 54	7.85	F0p	6.71±0.73	0.115	0.242	0.879	2.873	-0.016	0.027	8323	1.50	0.97	4459	07
11.	12211	02 00 33	+27 53 19	9	A7V	7.12±1.97	-	-	-	-	-	-	-	-	0.69	4399	07
															4.42	4401	07
															2.14	4402	07
12.	14433	02 21 55	+57 14 34	6.39	A1Ia	0.79±0.46	0.463	-0.088	0.913	2.606	-	-	-	-	1.98	2238	01
13.	15144	02 26 00	-15 20 28	5.86	A6Vsp	12.98±0.74	0.402	0.213	0.298	2.584	-	-	-	-	1.86	4085	06
14.	15550	02 30 38	+19 51 19	6.14	A9V	15.14±0.46	0.156	0.187	0.835	2.776	-	-	-	-	1.54	4431	07
15.	16145	02 35 04	-17 17 22	7.64	Ap	4.33±0.71	0.028	0.201	1.057	-	-	-	-	-	1.41	4087	06
															1.99	4088	06
															1.92	4089	06
															1.92	4090	06
16.	17034	02 45 42	+48 08 37	8.63	B8V+	0.92±0.90	-	-	-	-	-	-	-	-	1.68	4427	07
17.	17835	02 51 52	+02 54 49	8.9	A4	-	0.16	0.17	0.96	2.84	-	-	-	-	0.91	2216	01
18.	18078	02 56 32	+56 10 41	8.30	A0p	-	0.087	0.251	1.079	2.831	-0.044	0.243	7947	-	0.96	4459	07
19.	18610	02 54 18	-73 27 10	8.14	Ap	4.69±0.54	0.114	0.347	0.617	-	-	-	-	-	2.03	4098	06
															2.03	4101	06
20.	20880	03 16 08	-73 32 56	7.95	Ap	-	0.094	0.208	1.030	-	-	-	-	-	1.86	4092	06
21.	21746	03 30 00	-12 28 39	9.41	K0/K1IV	-	-	-	-	-	-	-	-	-	1.07	3659	05
22.	21985	03 32 25	-03 18 48	8.3	A1V	5.63±0.83	0.113	0.16	0.952	2.856	-	-	-	-	2.94	4104	07
															2.27	4108	07
23.	22374	03 36 58	+23 12 40	6.72	A2p	7.65±0.46	0.069	0.178	1.091	2.879	0.022	0.163	8397	1.70	2.63	4750	08
24.	22488	03 32 46	-66 43 46	7.50	Ap	4.39±0.45	-	-	-	-	-	-	-	-	1.93	4092	06
25.	23207	03 42 44	-18 42 50	7.54	Ap	4.83±0.71	0.106	0.259	0.856	-	-	-	-	-	1.96	4091	06
26.	23393	03 44 29	-12 03 31	8.30	F0III	4.35±0.91	0.222	0.164	0.772	2.753	0.024	0.133	7271	1.36	1.96	4094	06
27.	24825	03 55 16	-38 45 33	6.81	B9	4.23±0.33	-0.039	0.173	1.083	2.835	0.035	0.241	9683	1.99	1.34	4077	06
28.	25154	03 59 48	-00 01 12	9.88	A5	6.74±1.41	-	-	-	-	-	-	-	-	1.21	4397	07
29.	25487	04 03 54	+28 07 33	8.08	B8V	4.82±0.99	-	-	-	-	-	-	-	-	0.98	4459	07

Table 3. continued.

S.N.	Star HD	α_{2000}	δ_{2000}	m_v mag	Sp. Type	π mas	b-y mag	m_1 mag	c_1 mag	β mag	δm_1 mag	δc_1 mag	T_{eff} K	$\log(L/L_\odot)$	Δt hr	HJD	Year of Observation
30.	25999	04 08 18	+32 27 36	7.51	Ap	6.11±0.85	-	-	-	-	-	-	-	-	1.15	4815	09
															1.52	4869	09
															1.43	4870	09
31.	27463	04 16 21	-60 56 54	6.36	Ap	7.92±0.42	0.022	0.224	0.890	2.874	-0.023	-0.028	9214	1.61	1.78	4091	06
32.	28430	04 27 22	-40 11 50	8.20	Ap	2.52±0.61	-	-	-	-	-	-	-	-	1.89	4094	06
33.	29578	04 36 31	-54 37 16	8.51	Ap	3.74±0.61	-	-	-	-	-	-	-	-	1.93	4095	06
34.	31225	04 53 12	-20 46 19	7.02	Ap	5.32±0.68	0.093	0.19	1.079	-	-	-	-	-	2.33	4088	06
															1.91	4089	06
															1.38	4090	06
35.	34060	05 12 03	-49 03 37	7.82	B9Vp	2.74±0.48	-	-	-	-	-	-	-	-	1.91	4095	06
36.	34162	05 15 31	+05 45 35	8.68	F0	4.79±1.13	0.148	0.186	0.935	2.834	0.027	0.153	7982	1.15	1.34	4400	07
37.	34205	05 15 06	-15 06 01	9.32	Ap	-	0.135	0.215	0.962	2.911	-	-	-	-	1.60	2288	02
															1.59	2289	02
															1.92	2296	02
															2.14	2683	03
															2.24	2686	03
															2.21	2693	03
38.	35450	05 28 24	+58 40 29	8.16	A3	7.42±0.87	-	-	-	-	-	-	-	-	1.48	4397	07
39.	36955	05 35 04	-01 24 06	9.58	A2	-	0.057	0.198	0.848	2.866	0.005	-0.054	8270	-	1.08	4427	07
40.	37308	05 36 53	-17 00 59	8.71	A	-	-	-	-	-	-	-	-	-	1.78	4096	06
41.	38719	05 44 20	-56 54 58	7.50	Ap	4.19±0.45	0.011	0.206	1.038	-	-	-	-	-	2.19	4095	06
42.	38817	05 50 37	+44 00 41	7.56	A2	7.27±0.76	0.066	0.217	0.942	2.860	-0.012	0.052	8209	1.50	1.51	4071	06
43.	39082	05 50 24	+04 57 24	7.42	B9	6.63±0.53	-0.027	0.220	0.887	2.873	-0.019	-0.029	10451	2.42	1.16	4428	07
44.	39575	05 52 24	-26 17 28	7.83	A0	4.08±0.70	-0.074	0.267	0.905	-	-	-	-	-	2.15	4098	06
45.	40277	05 51 26	-70 28 46	8.33	Ap	4.45±0.60	0.041	0.239	0.901	-	-	-	-	-	1.99	4102	07
46.	40886	06 00 28	-27 53 18	8.21	A0	0.83±0.74	-	-	-	-	-	-	-	-	2.06	4096	06
47.	41089	06 00 51	-42 52 14	6.57	B9IIIp	4.25±0.29	-	-	-	-	-	-	-	-	3.03	4092	06
48.	41511	06 04 59	-16 29 04	4.97	A1V	3.59±0.31	0.186	0.030	1.323	2.775	0.164	0.593	9377	3.18	1.99	4103	07
49.	41786	06 08 02	+21 17 44	7.29	F0	9.70±1.09	0.193	0.275	0.690	2.782	-0.078	0.000	7557	2.30	1.11	4101	06
50.	42326	06 09 17	-17 17 30	7.70	Ap	6.66±0.66	0.008	0.231	0.922	-	-	-	-	-	2.48	4091	06
51.	43901	06 16 14	-47 49 46	8.20	Ap	1.44±0.46	0.132	0.228	0.946	2.860	-0.023	0.056	8208	2.35	1.99	4097	06
52.	44195	06 20 42	+05 16 42	7.54	F0	11.22±0.75	0.179	0.188	0.705	2.753	-	-	-	-	1.96	2285	02
53.	44903	06 25 20	+23 03 24	8.36	A5	-	0.069	0.204	0.979	2.867	-	-	-	-	1.17	2285	02
54.	45297	06 26 42	+03 52 18	9.23	B9	-	-	-	-	-	-	-	-	-	2.19	4165	07
55.	45698	06 27 11	-37 06 07	8.15	A2	5.60±0.56	0.069	0.244	0.846	-	-	-	-	-	1.99	4101	06
56.	47311	06 40 01	+42 33 55	8.71	F0	3.76	0.217	0.204	0.756	2.746	-	-	-	-	1.78	1943	01
57.	48953	06 46 49	+16 46 20	6.8	F5	10.39	0.247	0.308	0.623	2.752	-	-	-	-	1.10	2210	01
															0.91	2305	02
58.	51496	07 00 57	+56 51 13	9.83	F5	-	-	-	-	-	-	-	-	-	2.01	4106	07
59.	51684	06 56 29	-40 59 25	7.94	Ap	3.58±0.60	0.154	0.248	0.768	2.832	-	-	-	-	2.10	4088	06
60.	55719	07 12 16	-40 29 56	5.31	A3spe	7.93±0.38	0.012	0.217	1.030	2.880	-0.017	0.100	9101	2.28	2.09	4102	07
61.	56148	07 19 48	+61 35 29	9.00	F0	-	0.204	0.178	0.628	2.722	0.000	0.044	7046	-	1.05	4104	07
62.	56350	07 13 40	-53 40 04	6.69	Ap	6.61±0.26	-	-	-	2.799	-	-	-	-	2.45	4096	06
63.	61763	07 38 47	-44 49 48	7.94	Apsh	2.54±0.41	-	-	-	-	-	-	-	-	2.35	4097	06
64.	66195	07 56 47	-70 42 59	8.65	Ap	5.17±0.76	0.043	0.227	0.886	-	-	-	-	-	2.03	4103	07
65.	70338	08 21 53	+13 37 26	7.32	A2	5.51±0.76	0.173	0.271	0.805	2.814	-	-	-	1.45	0.93	2338	02
66.	72611	08 32 17	-41 49 56	7.01	Ap	5.61±0.42	-0.062	0.192	0.748	-	-	-	-	-	2.27	4098	06
															0.96	4101	06

Table 3. continued.

S.N.	Star HD	α_{2000}	δ_{2000}	m_v mag	Sp. Type	π mas	b-y mag	m_1 mag	c_1 mag	β mag	δm_1 mag	δc_1 mag	T_{eff} K	$\log(L/L_\odot)$	Δt hr	HJD	Year of Observation
67.	72634	08 29 43	-67 08 23	7.27	Ap	3.35±0.45	-0.011	0.185	1.025	-	-	-	-	-	2.01	4103	07
68.	72943	08 36 08	+15 18 49	6.32	F0IV	12.86±0.45	0.211	0.186	0.732	2.720	-0.009	0.152	6991	1.16	1.13	4099	06
69.	73095	08 37 35	+31 50 31	8.85	A3	-	0.19	0.195	0.702	2.746	-	-	-	-	0.96	2239	01
70.	73345	08 38 38	+19 59 23	8.14	F0V	-	0.121	0.210	0.883	2.812	-0.004	0.140	7780	-	1.19	4429	07
71.	73574	08 39 43	+20 05 11	7.75	A5V	-	0.127	0.207	0.871	2.799	-0.004	0.093	7659	-	2.47	4164	07
															1.61	4166	07
72.	74067	08 40 19	-40 15 50	5.20	B9V	11.68±0.50	-0.050	0.220	0.898	2.846	-0.013	0.036	10412	-	2.38	4102	07
73.	75445	08 48 42	-39 14 01	7.12	A3	9.23±0.45	0.159	0.218	0.729	-	-	-	-	-	2.80	2288	02
															1.45	2289	02
															1.97	2296	02
															1.99	2704	03
															2.04	2709	03
															2.16	2710	03
74.	76444	08 57 07	+29 12 57	9.11	F0	3.11±1.02	0.176	0.191	0.752	2.745	-0.006	0.128	7204	1.27	1.44	4104	07
75.	78388	09 09 52	+49 49 56	7.61	F0III	9.25±0.66	0.231	0.172	0.710	2.709	0.002	0.153	6900	0.92	2.28	4103	07
76.	82417	09 30 22	-46 48 48	9.24	Ap	-	-	-	-	-	-	-	-	-	5.14	3483	05
77.	86170	09 56 45	-02 17 20	8.42	A2	3.20±0.98	0.074	0.226	0.929	-	-	-	-	-	1.39	4428	07
															1.77	4431	07
															1.55	4459	07
78.	88385	10 09 49	-56 44 53	8.09	Ap	4.85±0.55	0.006	0.23	0.863	2.822	-	-	-	-	1.94	4174	07
79.	88701	10 13 00	-37 30 12	9.27	B9	2.36±0.99	-	-	-	-	-	-	-	-	1.34	4175	07
80.	100809	11 36 14	+14 41 51	8.25	Am	7.12±0.85	0.1	0.269	0.856	2.845	-	-	-	-	1.41	2009	01
81.	104044	11 58 53	-43 22 55	9.57	Ap	-	-	-	-	-	-	-	-	-	0.91	3482	05
82.	106374	12 14 18	-33 46 44	7.37	A2	5.63±0.54	-	-	-	-	-	-	-	-	0.97	3482	05
83.	117044	13 27 30	+13 54 49	8.19	F0II	5.25±0.76	0.209	0.211	0.674	2.749	-0.025	0.043	7267	1.19	1.32	4104	07
84.	117290	13 30 13	-49 07 58	9.25	Ap	-	-	-	-	-	-	-	-	-	1.97	4174	07
															3.22	4175	07
															1.41	4178	07
															1.50	4179	07
															2.48	4180	07
															3.48	4181	07
85.	127608	14 33 47	-46 45 33	8.56	Ap	-	-	-	-	-	-	-	-	-	4.66	3515	05
86.	140220	15 44 10	-44 06 50	7.97	Ap	-	-	-	-	-	-	-	-	-	2.01	3483	05
87.	144897	16 09 51	-41 09 27	8.59	Ap	5.61±1.04	-	-	-	-	-	-	-	-	2.01	2507	02
															1.60	2511	02
															1.71	2513	02
															1.63	2516	02
															1.58	2520	02
88.	149769	16 40 47	-62 25 54	9.75	Ap	-	-	-	-	-	-	-	-	-	3.79	2123	01
89.	161423	17 52 02	-71 41 24	9.31	Ap	-	-	-	-	-	-	-	-	-	3.37	2127	01
															1.24	2128	01
90.	162639	17 54 41	-50 26 45	9.93	Ap	-	-	-	-	-	-	-	-	-	1.06	3482	05
91.	164258	18 00 15	+00 37 46	6.37	A3spe	7.39±0.52	0.087	0.181	1.099	2.905	-	-	-	-	0.53	3518	05
92.	168767	18 22 30	-26 54 40	8.71	A0	-	-	-	-	-	-	-	-	-	1.50	3482	05
93.	169380	18 26 06	-37 54 42	9.83	A3	-	-	-	-	-	-	-	-	-	2.02	2128	01
94.	170397	18 29 47	-14 34 55	6.02	Ap	9.54±0.36	-0.029	0.190	0.925	2.837	0.018	0.080	10447	3.85	1.98	4298	07
95.	172976	18 41 03	+44 16 16	7.29	F0III	5.03±0.48	0.181	0.234	0.827	2.788	-0.035	0.126	7578	1.62	2.03	4251	07
															1.11	4374	07

Table 3. continued.

S.N.	Star HD	α_{2000}	δ_{2000}	m_v mag	Sp. Type	π mas	b-y mag	m_1 mag	c_1 mag	β mag	δm_1 mag	δc_1 mag	T_{eff} K	$\log(L/L_\odot)$	Δt hr	HJD	Year of Observation
96.	173612	18 46 30	-08 25 58	9.08	A0	-	-	-	-	-	-	-	-	-	2.74	3515	05
97.	178892	19 09 55	+14 57 58	8.94	B9	4.53±1.10	-	-	-	-	-	-	-	-	0.86	4375	07
98.	183806	19 33 22	-45 16 18	5.58	Ap	8.22±0.40	-0.025	0.167	1.062	2.849	0.039	0.194	9816	2.01	2.59	4295	07
99.	187474	19 51 51	-39 52 28	5.32	Ap	10.82±0.88	-0.047	0.203	0.864	2.820	0.003	0.044	10706	1.93	3.20	4294	07
100.	188008	19 54 27	-36 34 32	8.86	A5	-	0.040	0.248	0.858	2.880	-0.048	-0.072	8797	-	1.43	4296	07
101.	190401	20 03 09	+41 28 28	6.99	Am	9.34±0.35	0.220	0.209	0.728	2.744	-0.026	0.059	7204	2.13	1.13	4374	07
															2.40	4375	07
															2.01	4376	07
102.	196604	20 36 50	+44 54 40	8.12	A3	8.04±0.70	0.222	0.218	0.633	2.737	-	-	-	-	1.07	1832	00
103.	204367	21 28 41	-25 38 39	7.83	A0	5.07±0.77	-	-	-	-	-	-	-	-	2.09	4295	07
104.	205087	21 32 27	+23 23 40	6.68	B9sp	5.87±0.36	-0.064	0.189	0.752	2.799	0.014	-0.589	11906	1.94	1.35	4428	07
105.	208759	22 00 54	-64 57 41	9.98	Ap	-	-	-	-	-	-	-	-	-	2.02	2127	01
															1.67	2128	01
106.	212385	22 24 38	-39 07 37	6.84	A2p	7.92±0.63	0.067	0.225	0.946	-	-	-	-	-	2.04	4294	07
107.	216018	22 49 26	-11 20 57	7.62	A7	8.03±0.66	0.165	0.318	0.561	-	-	-	-	-	1.35	2574	02
															2.50	2585	02
															2.69	2586	02
															2.24	2588	02
															2.16	2589	02
															2.17	2590	02
108.	290665	05 35 10	-00 50 13	9.44	B9	-	0.037	0.207	0.829	2.854	-0.001	-0.049	9167	-	1.34	4459	07
															1.94	4492	08

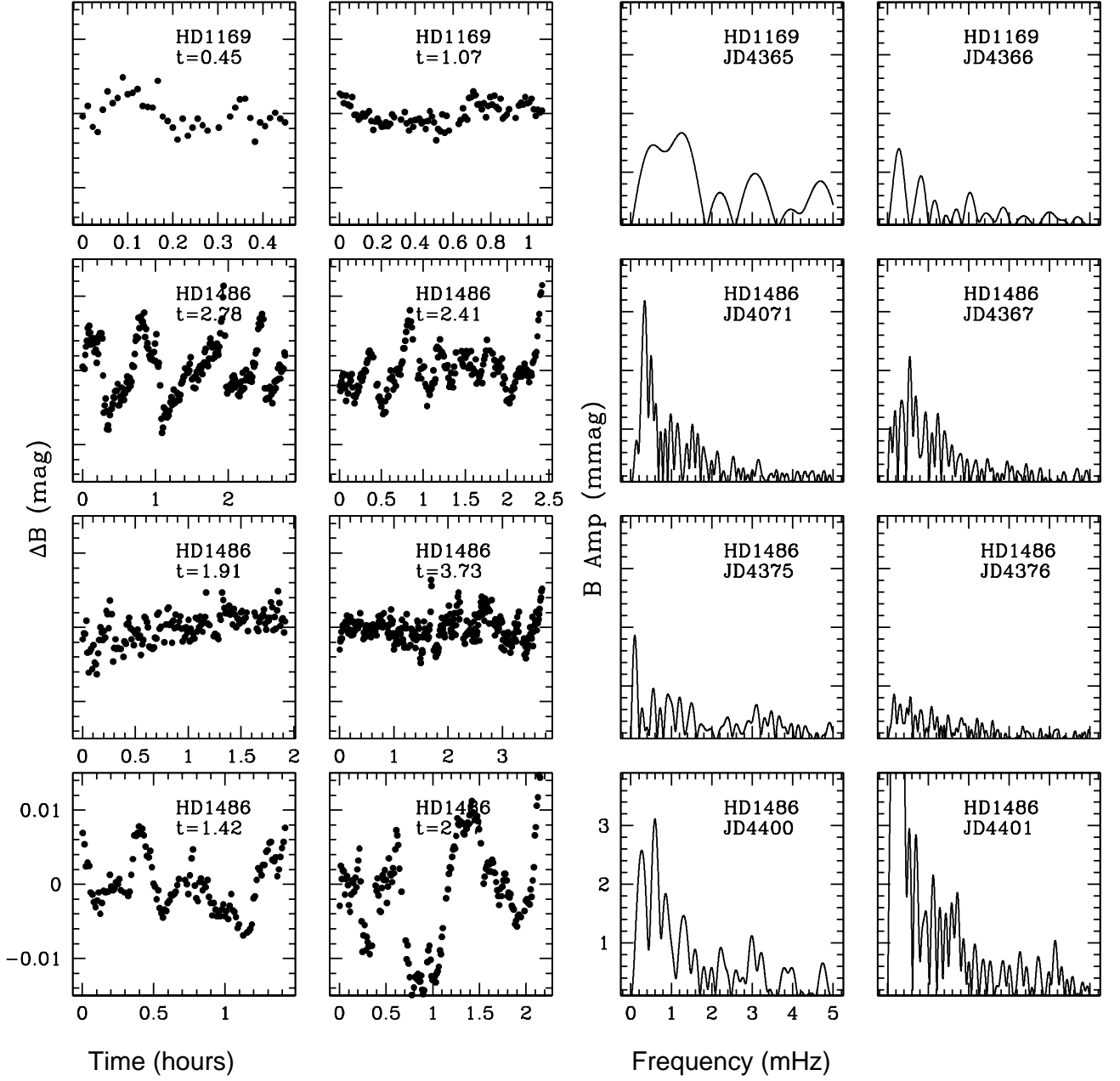


Fig. 3. The light curves (left columns) of the pulsation candidate stars observed from ARIES/SAAO and their corresponding pre-whitened amplitude spectra (right columns). The light curves have been binned to 40-sec integrations.

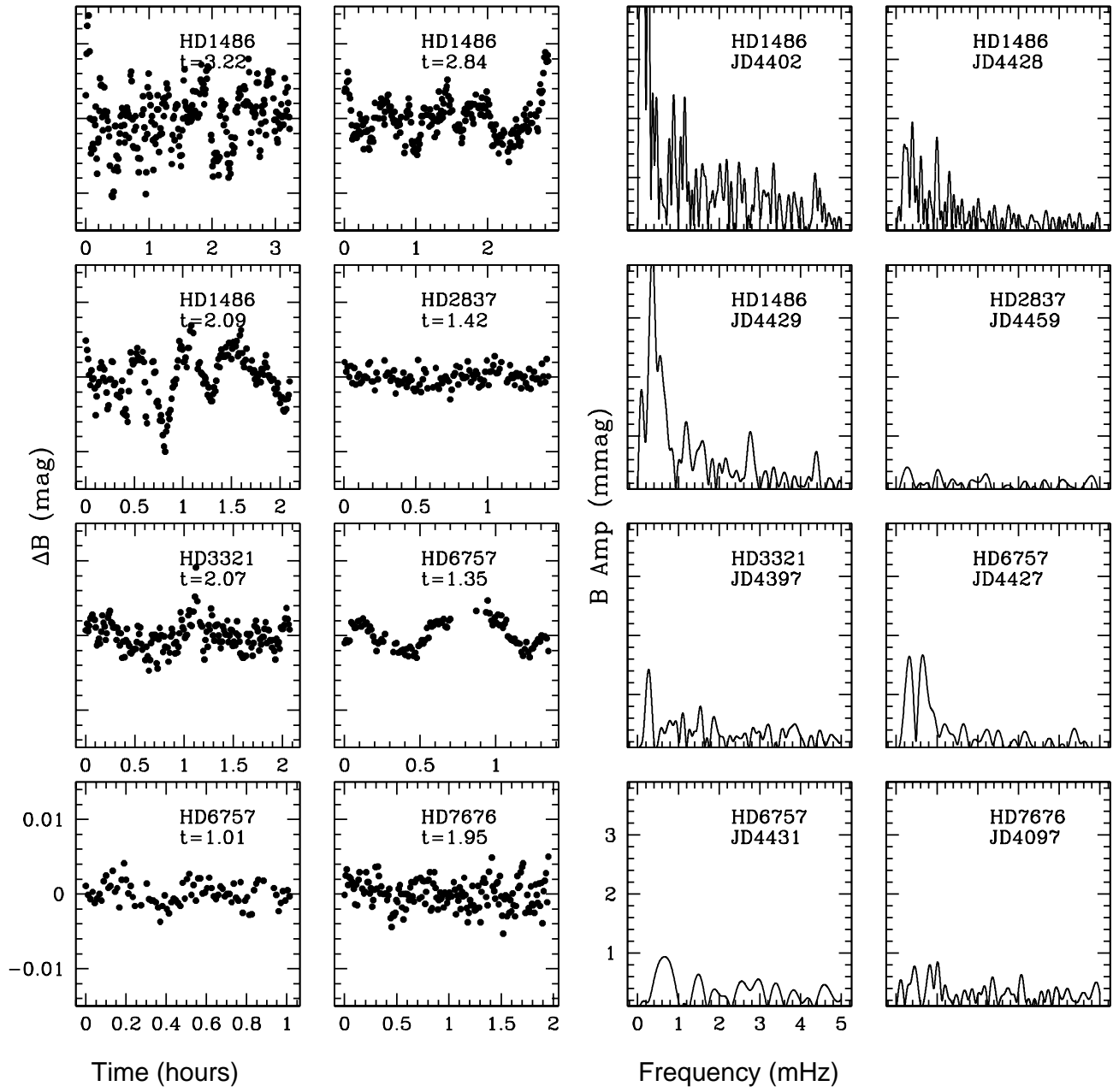


Fig. 3. Continued.

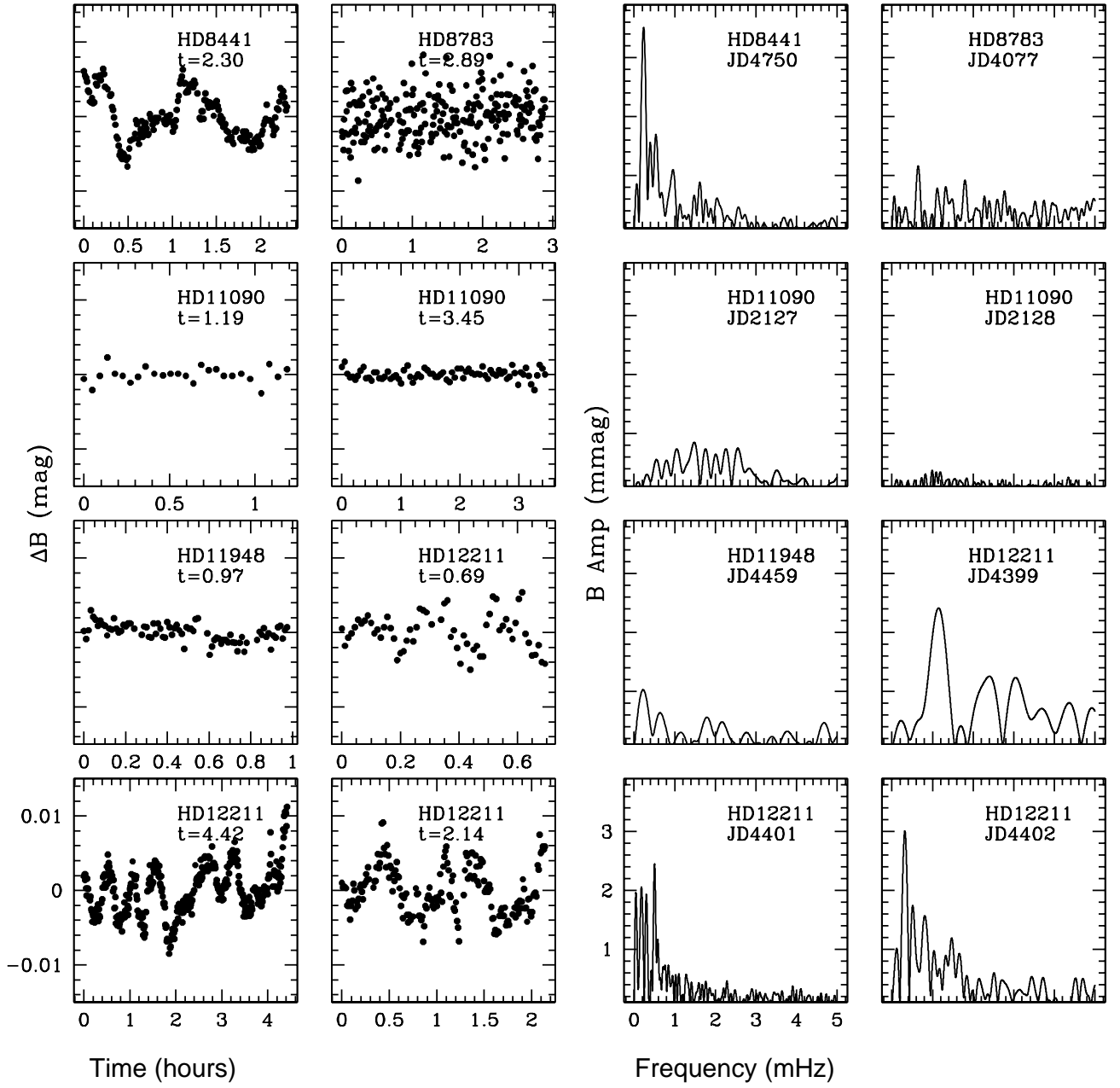


Fig. 3. Continued.

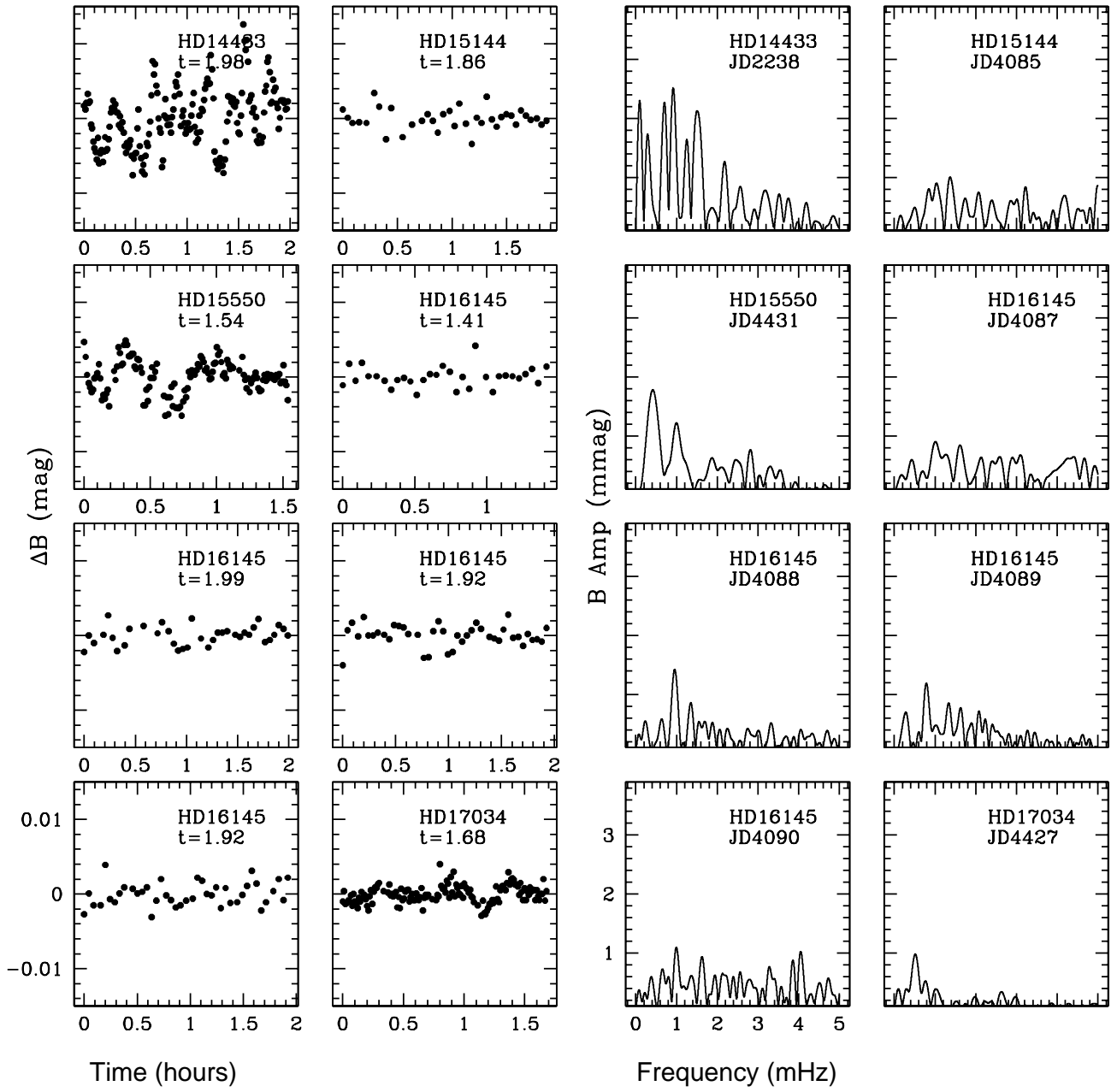


Fig. 3. Continued.

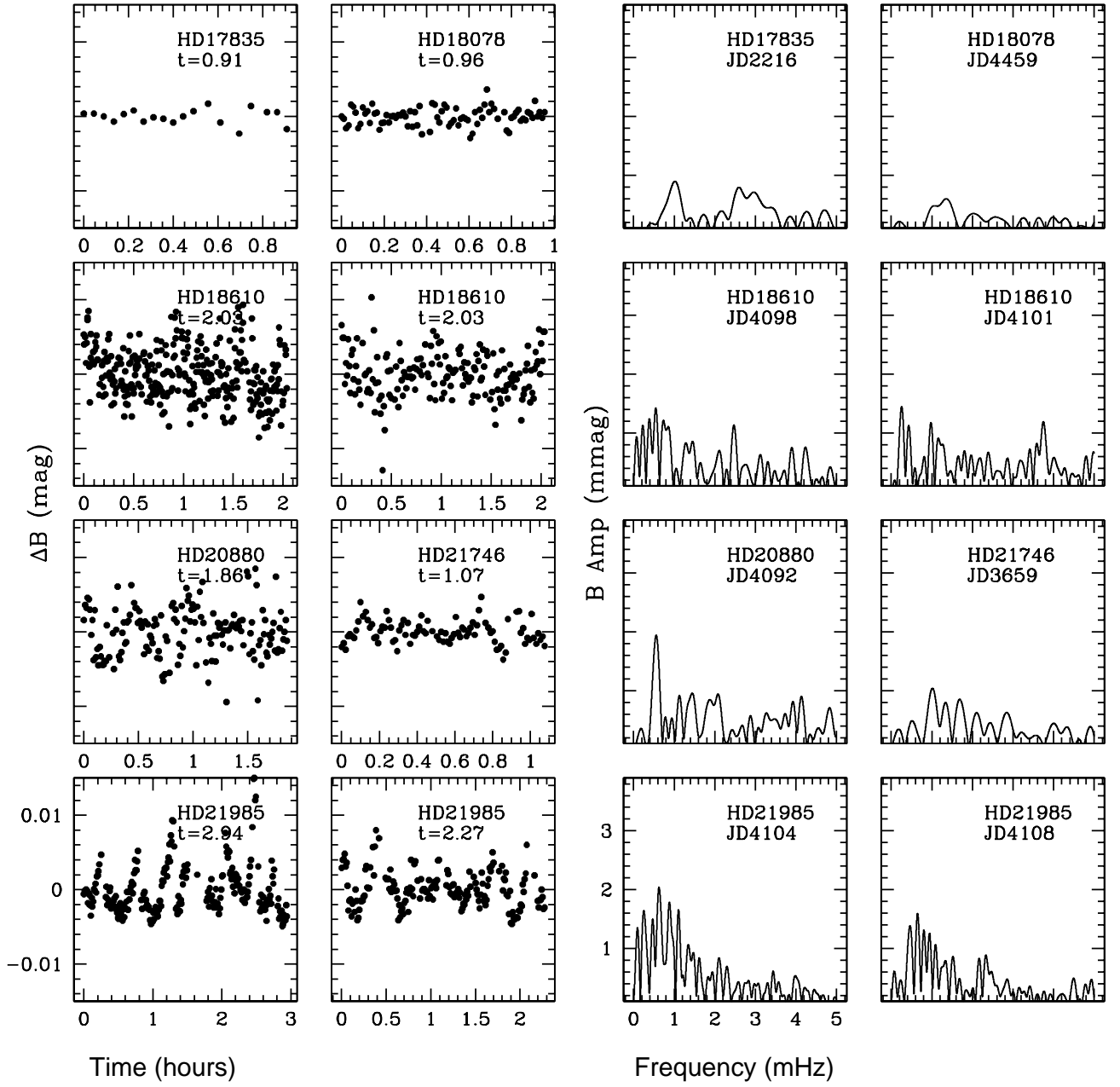


Fig. 3. Continued.

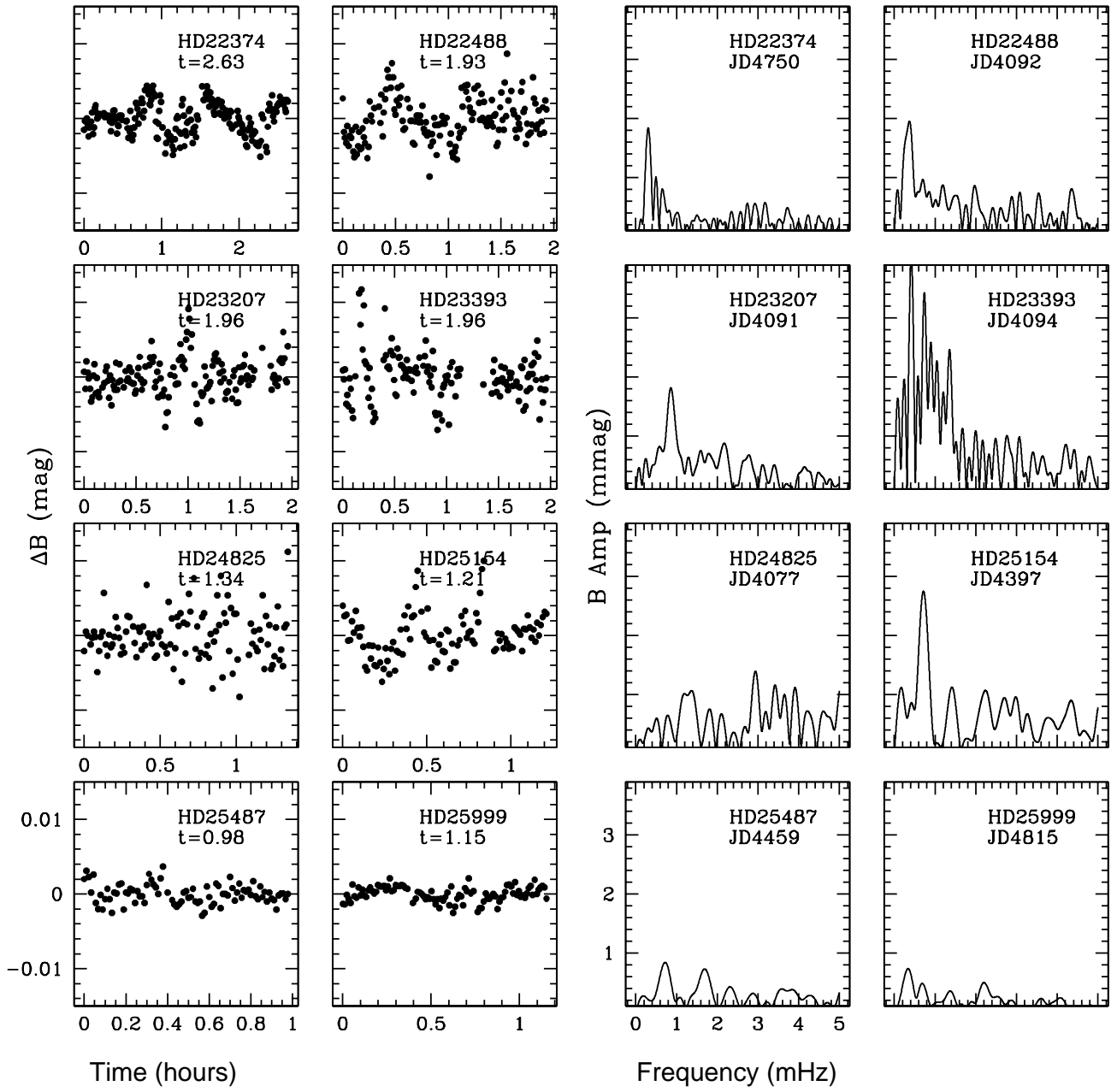


Fig. 3. Continued.

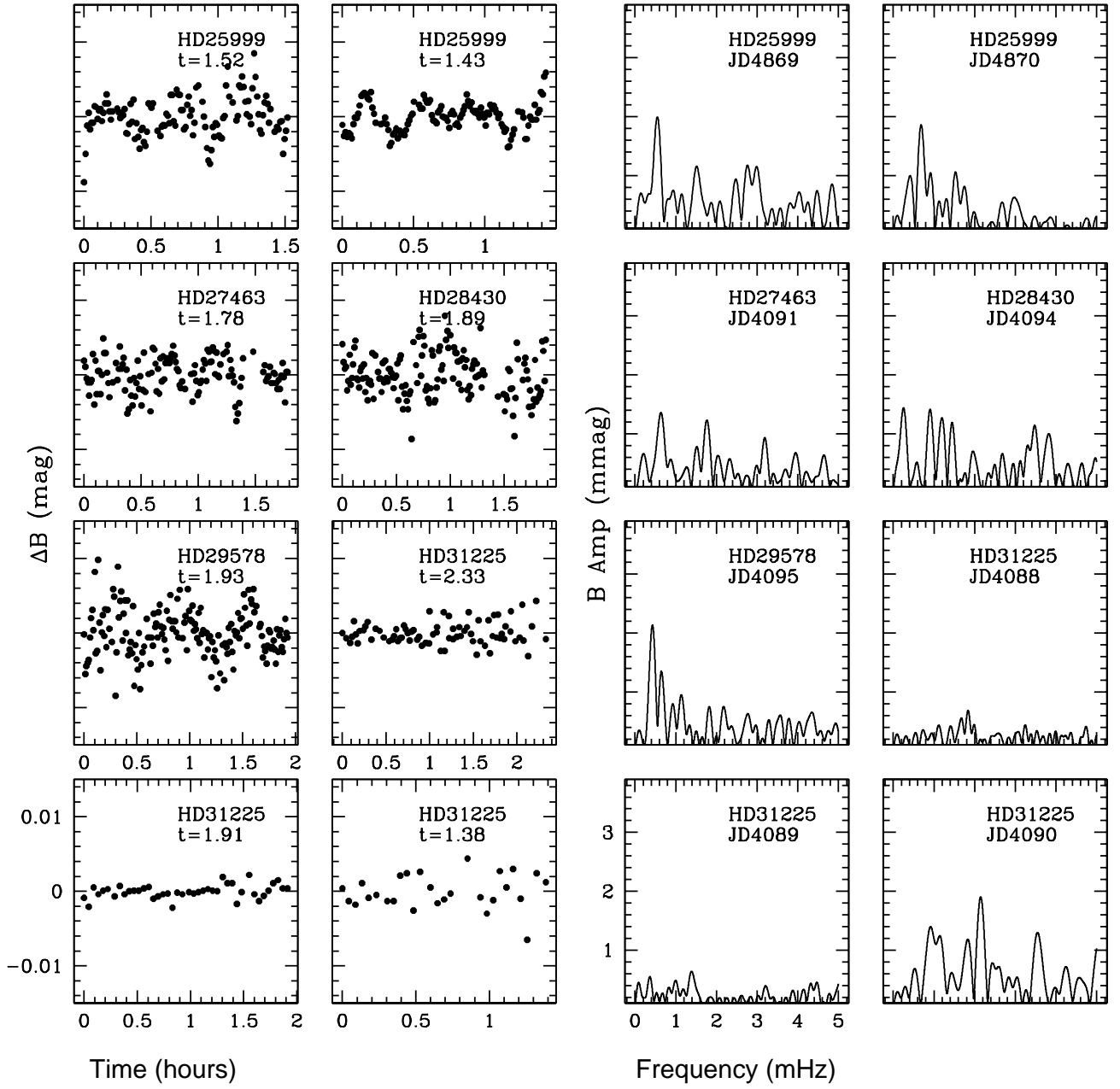


Fig. 3. Continued.

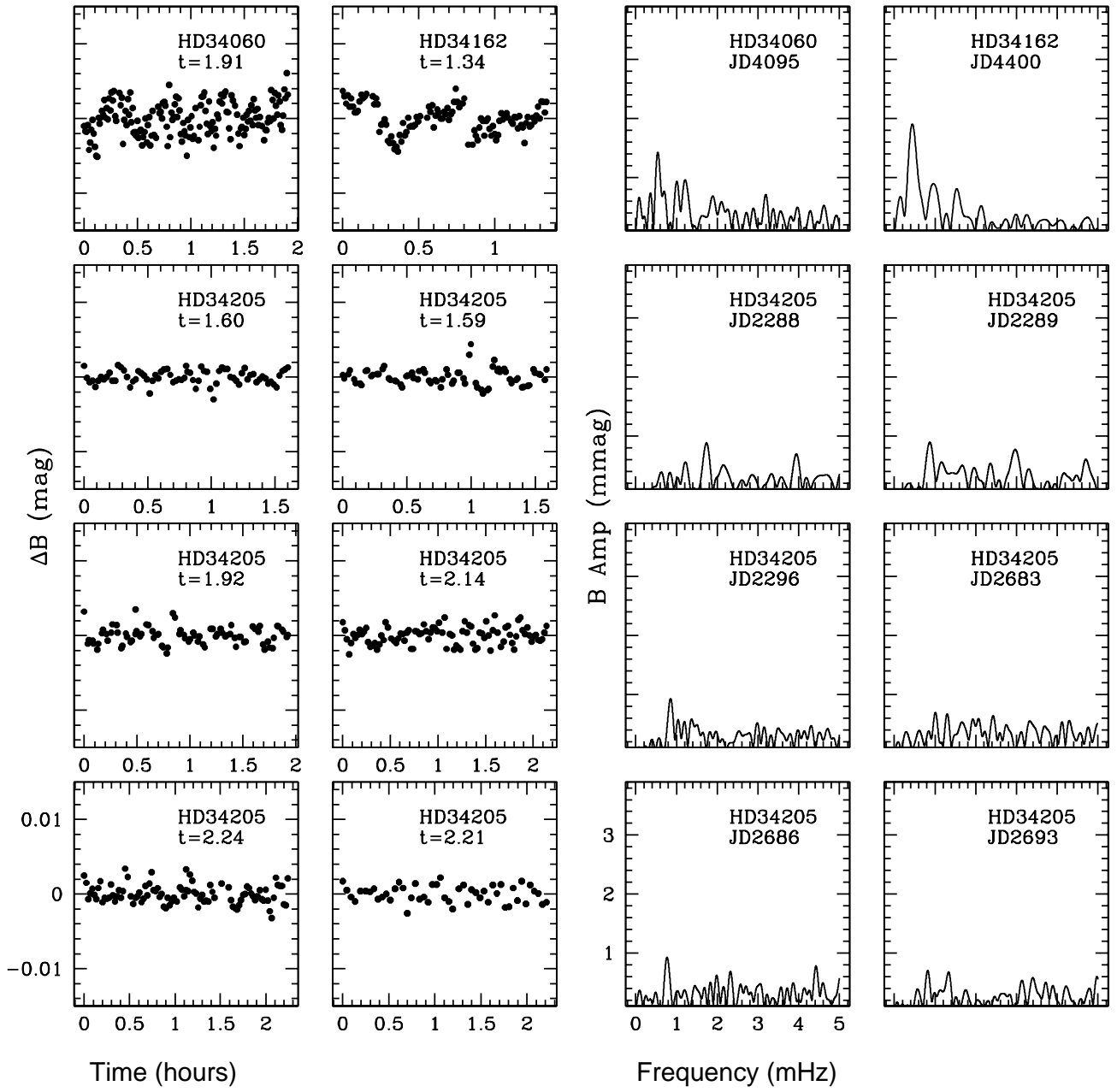


Fig. 3. Continued.

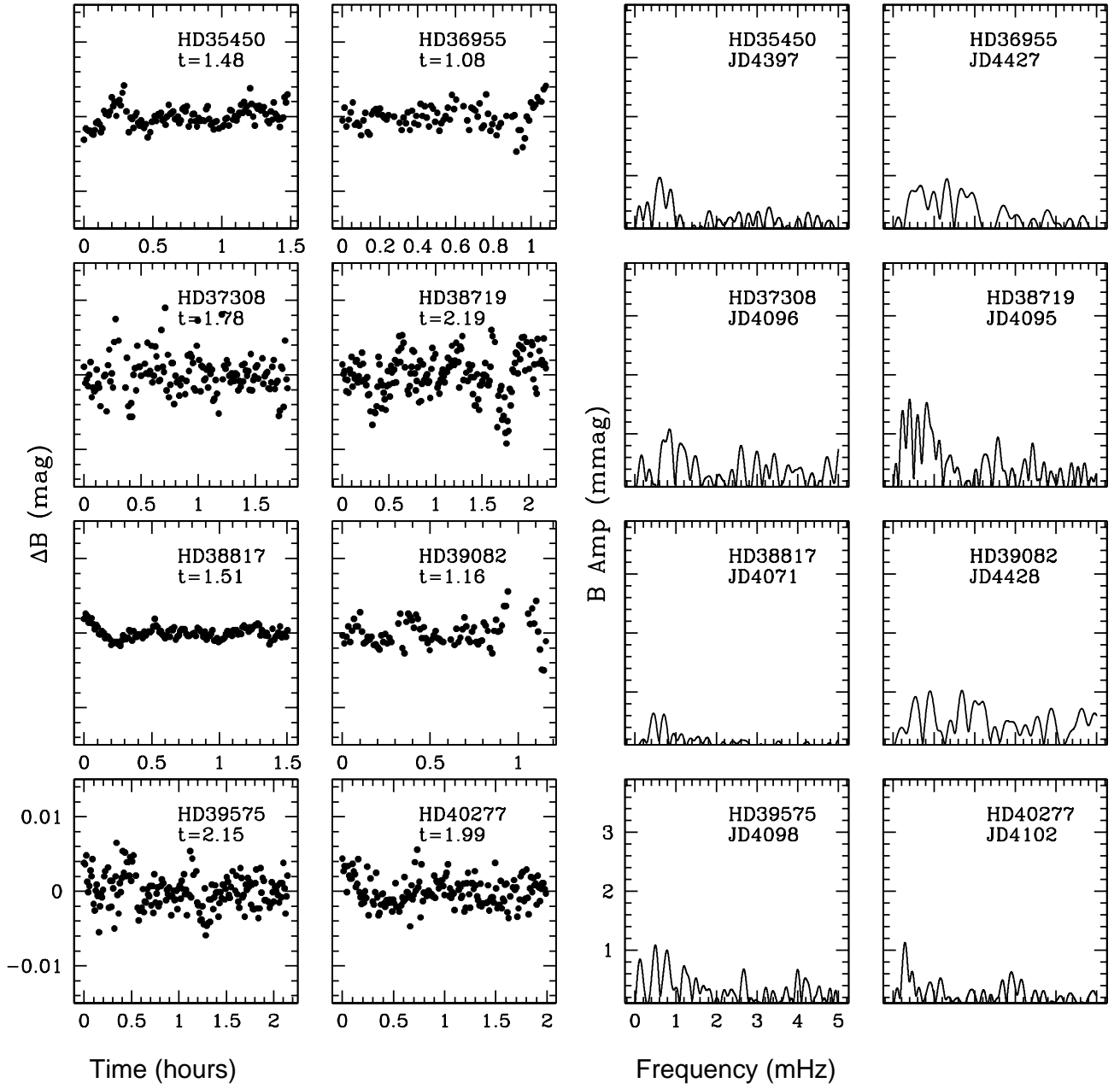


Fig. 3. Continued.

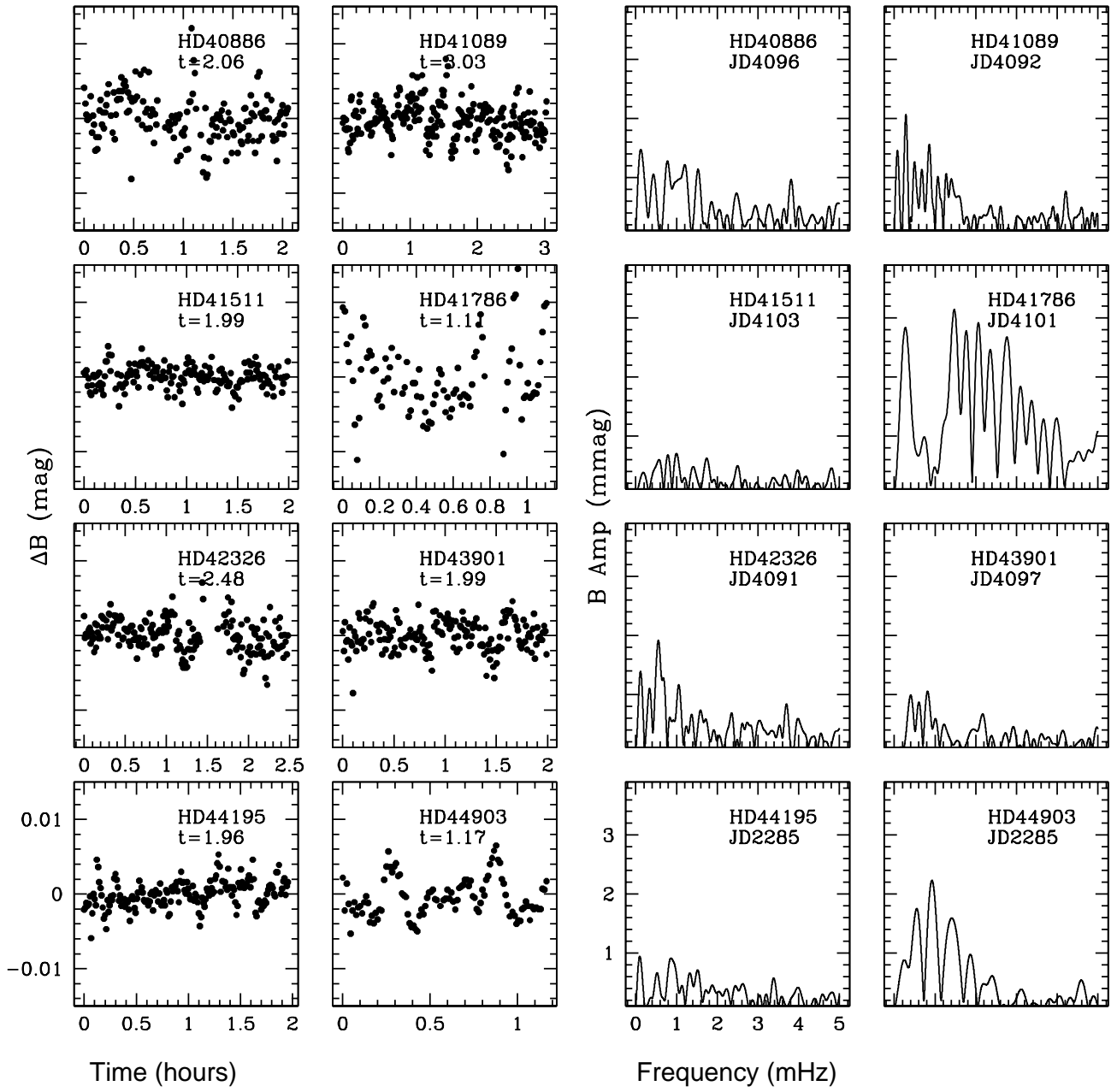


Fig. 3. Continued.

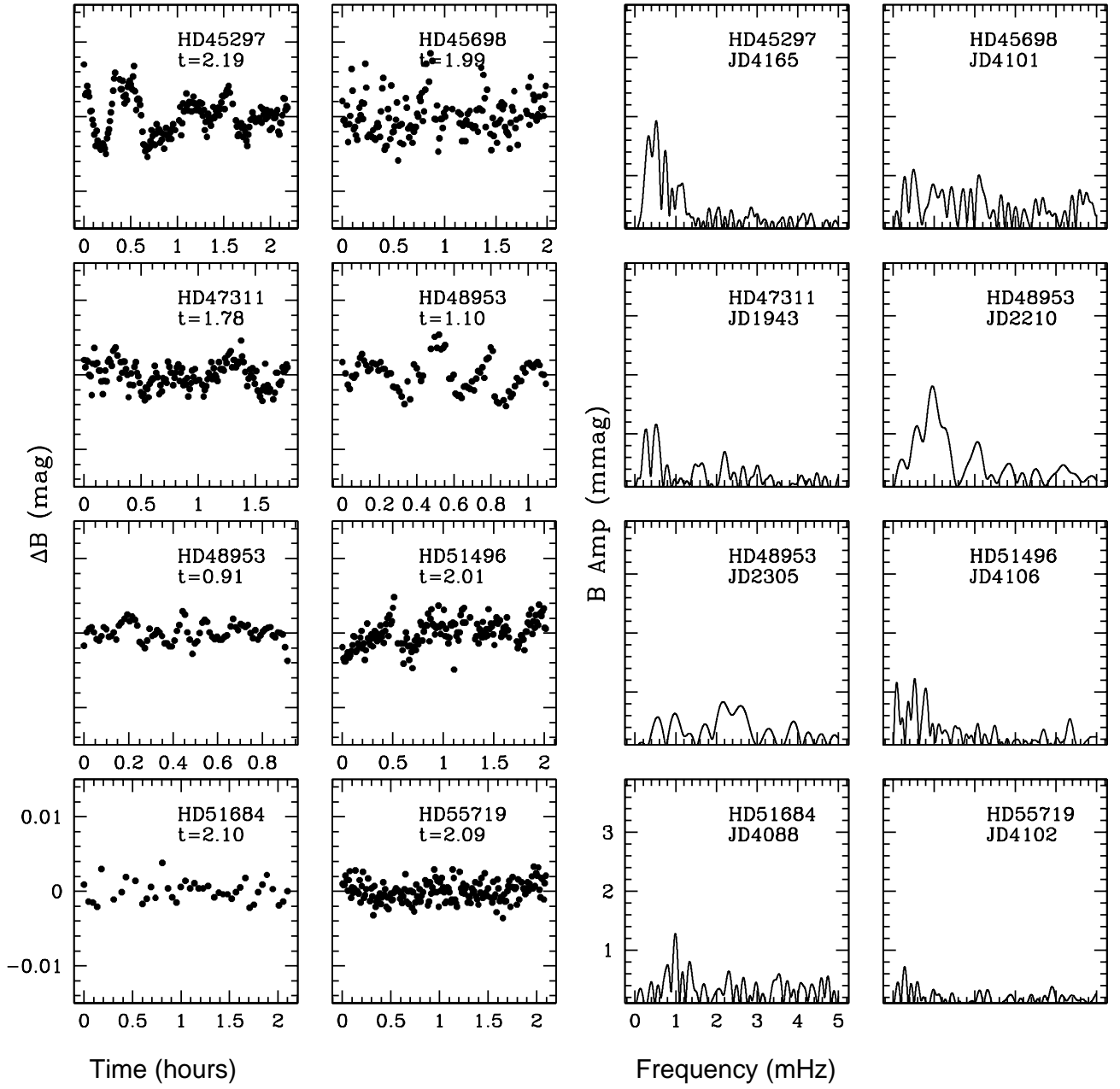


Fig. 3. Continued.

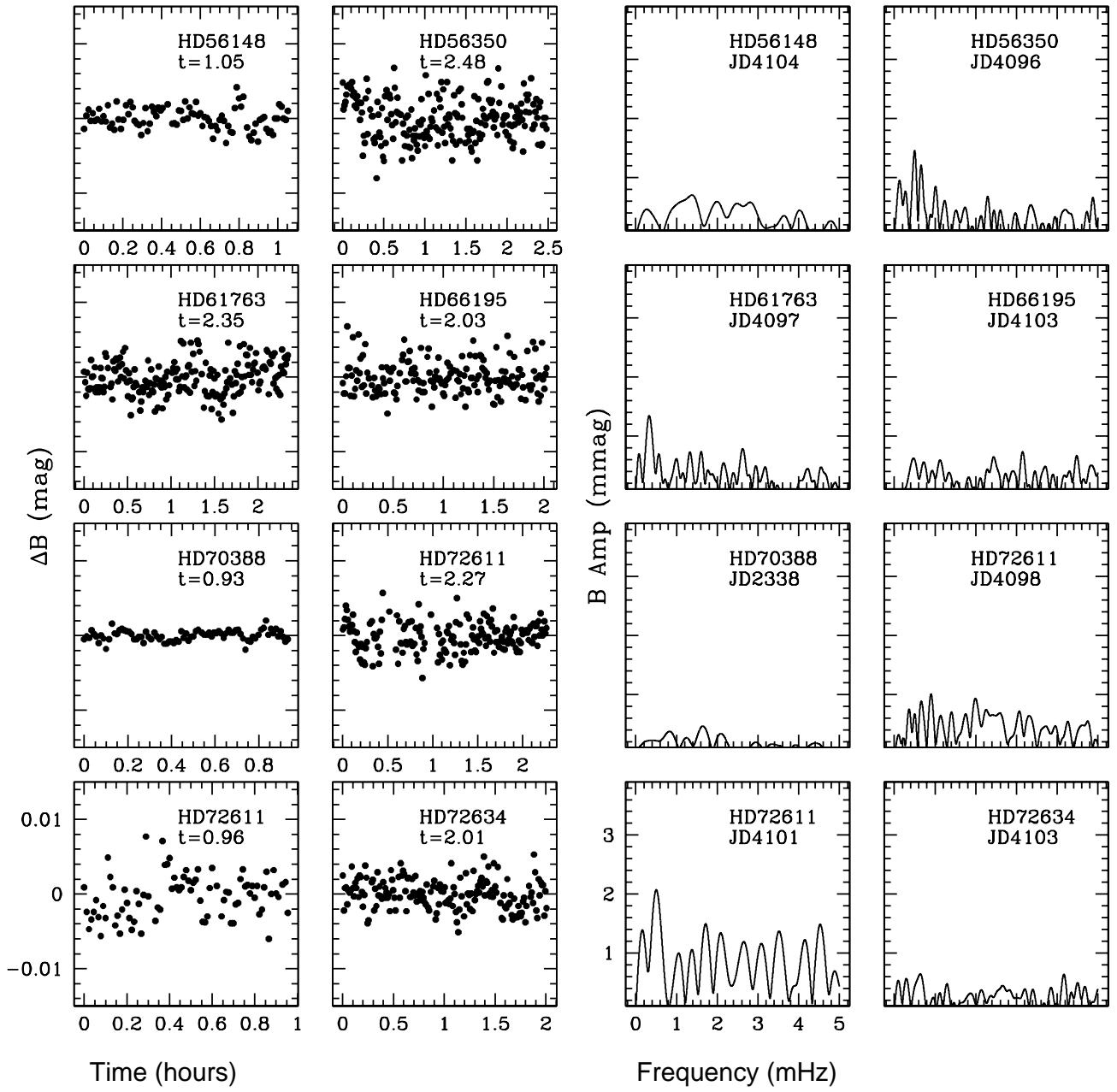


Fig. 3. Continued.

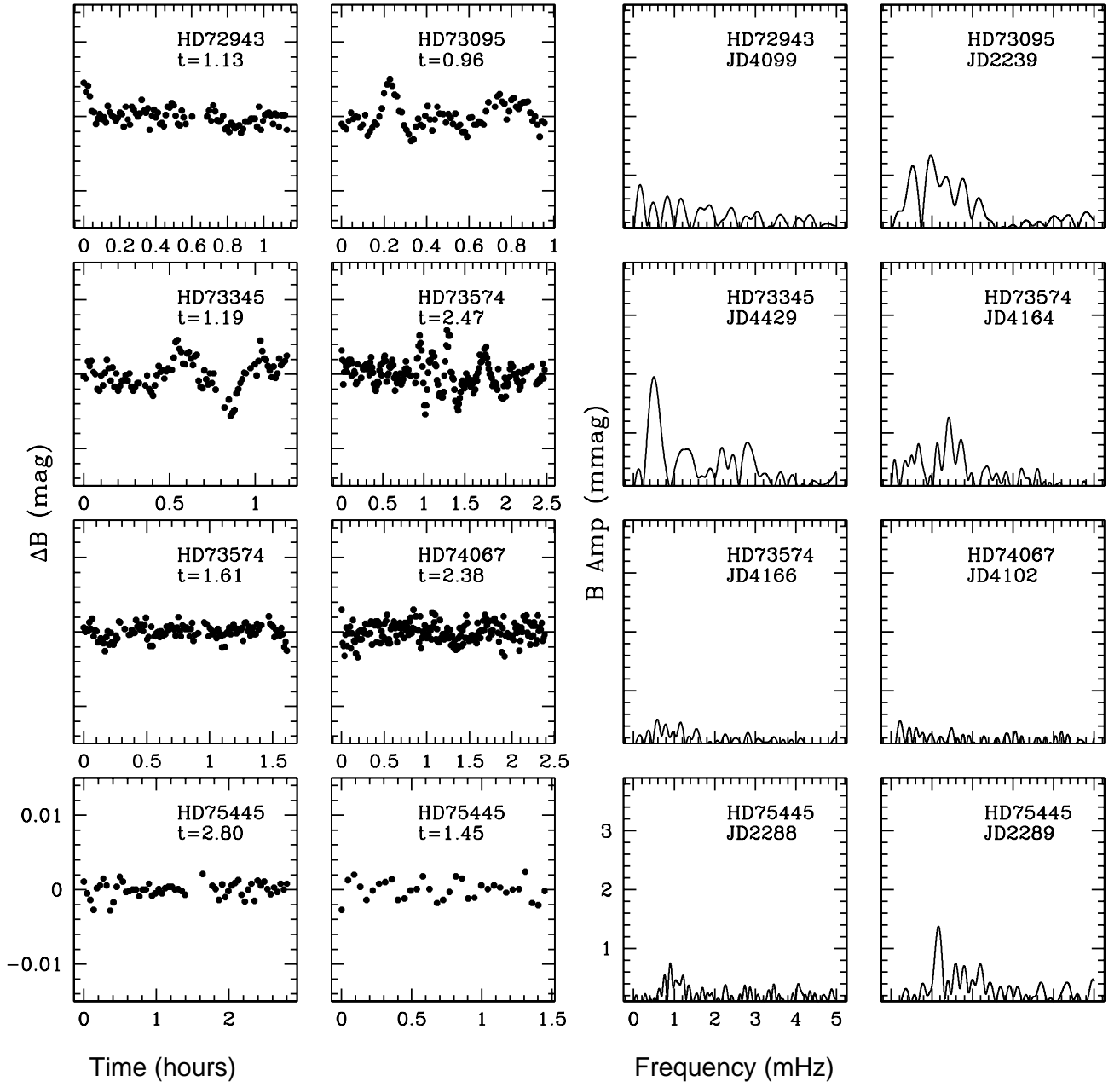


Fig. 3. Continued.

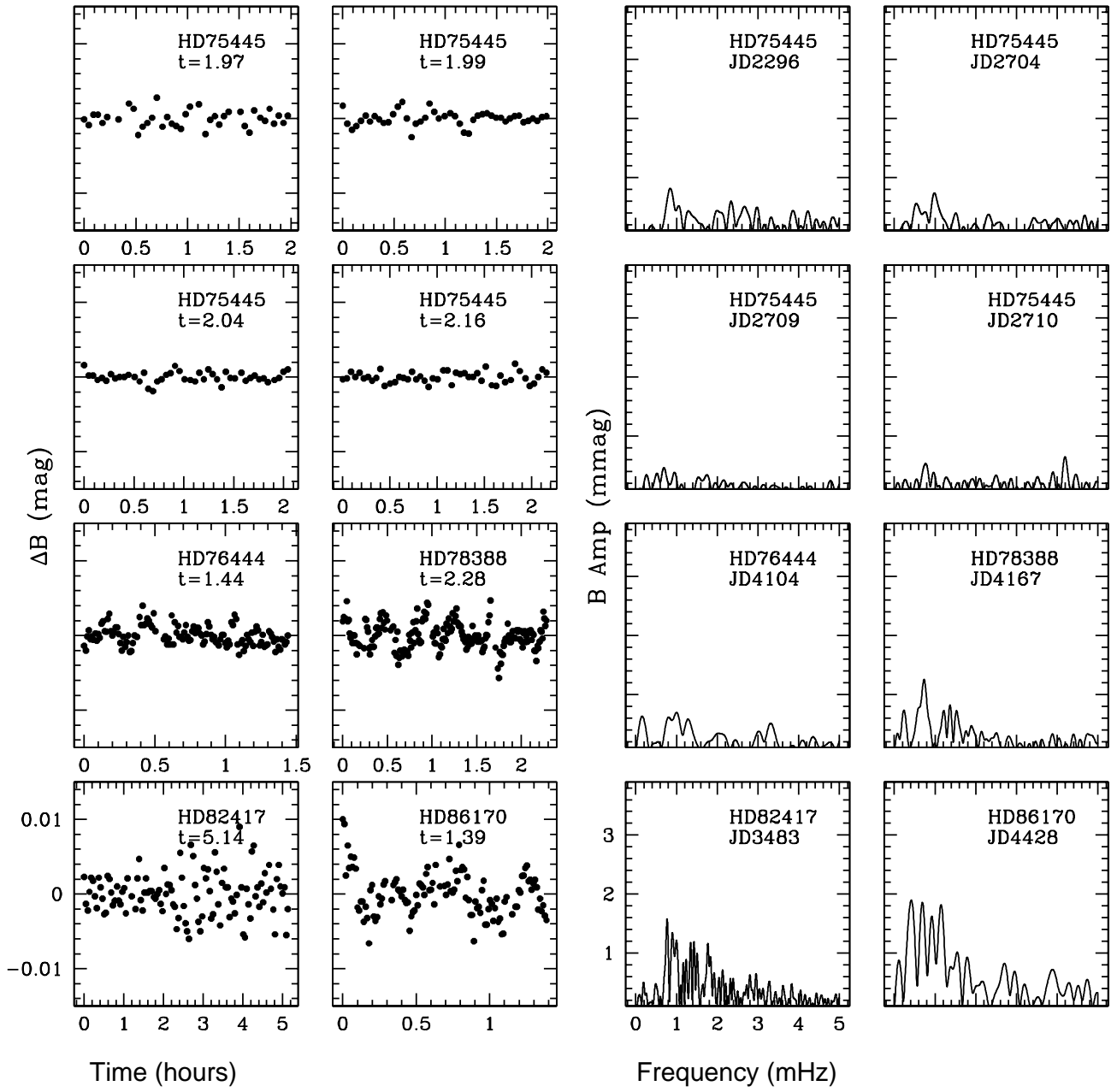


Fig. 3. Continued.

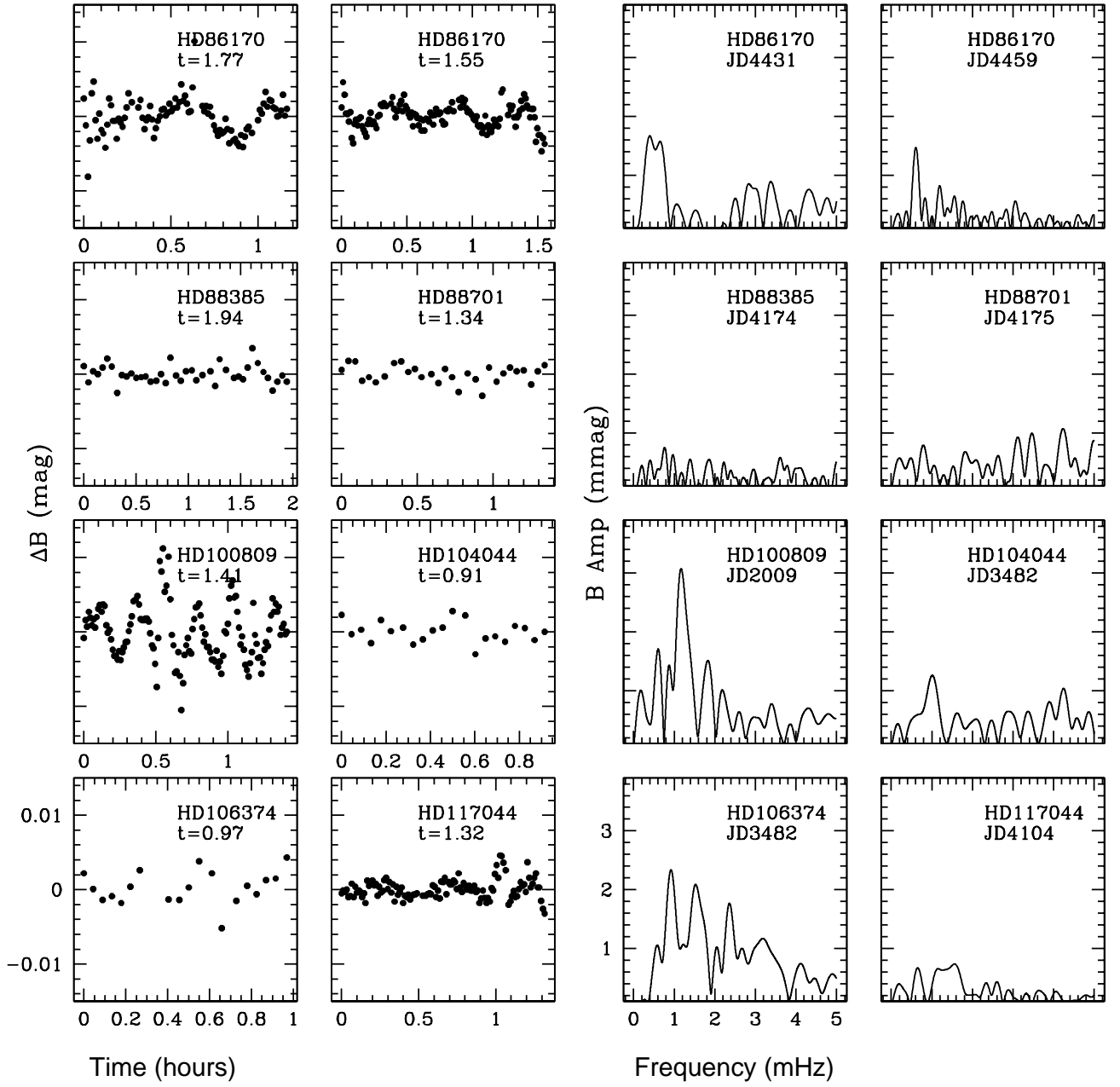


Fig. 3. Continued.

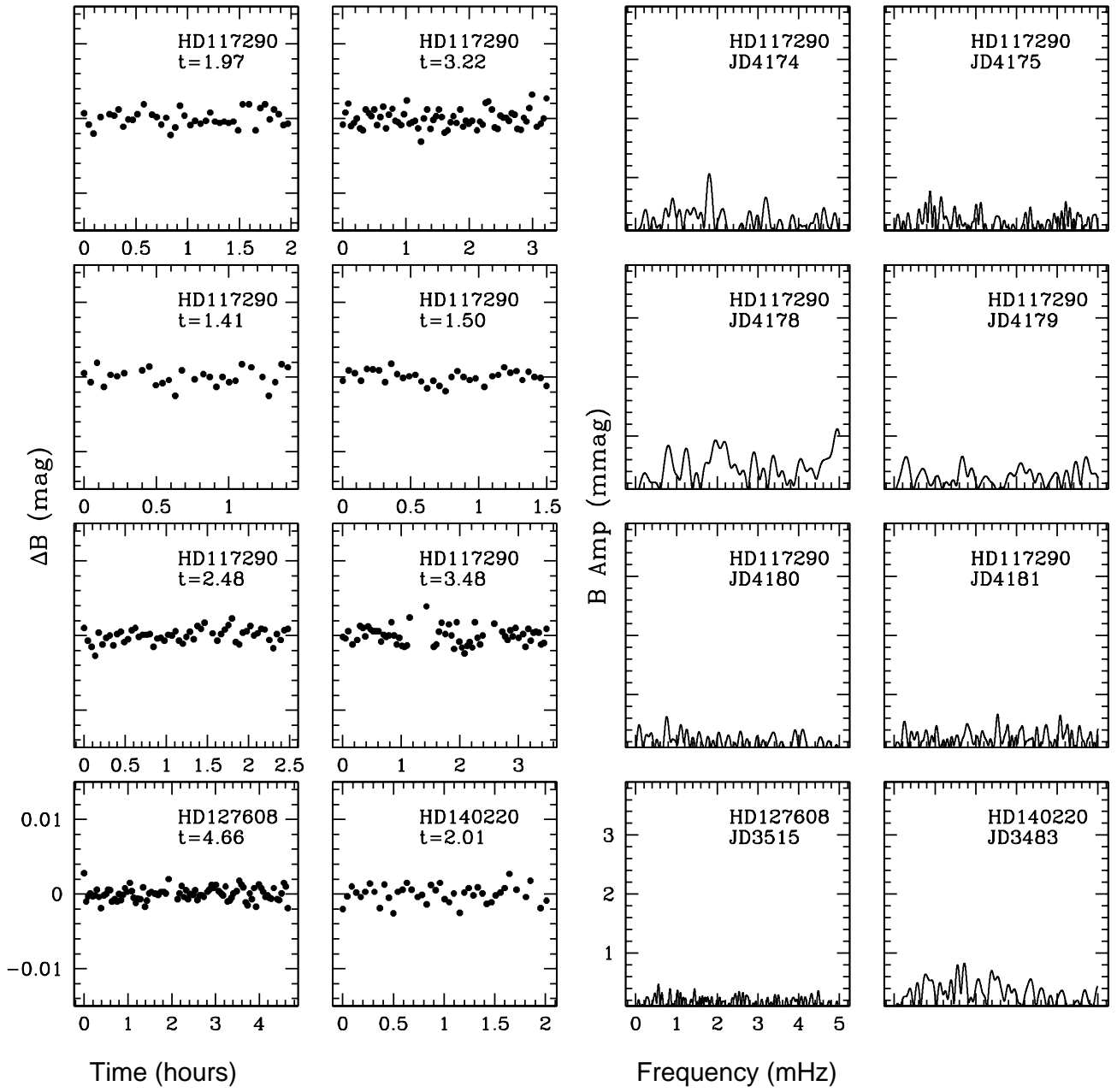


Fig. 3. Continued.

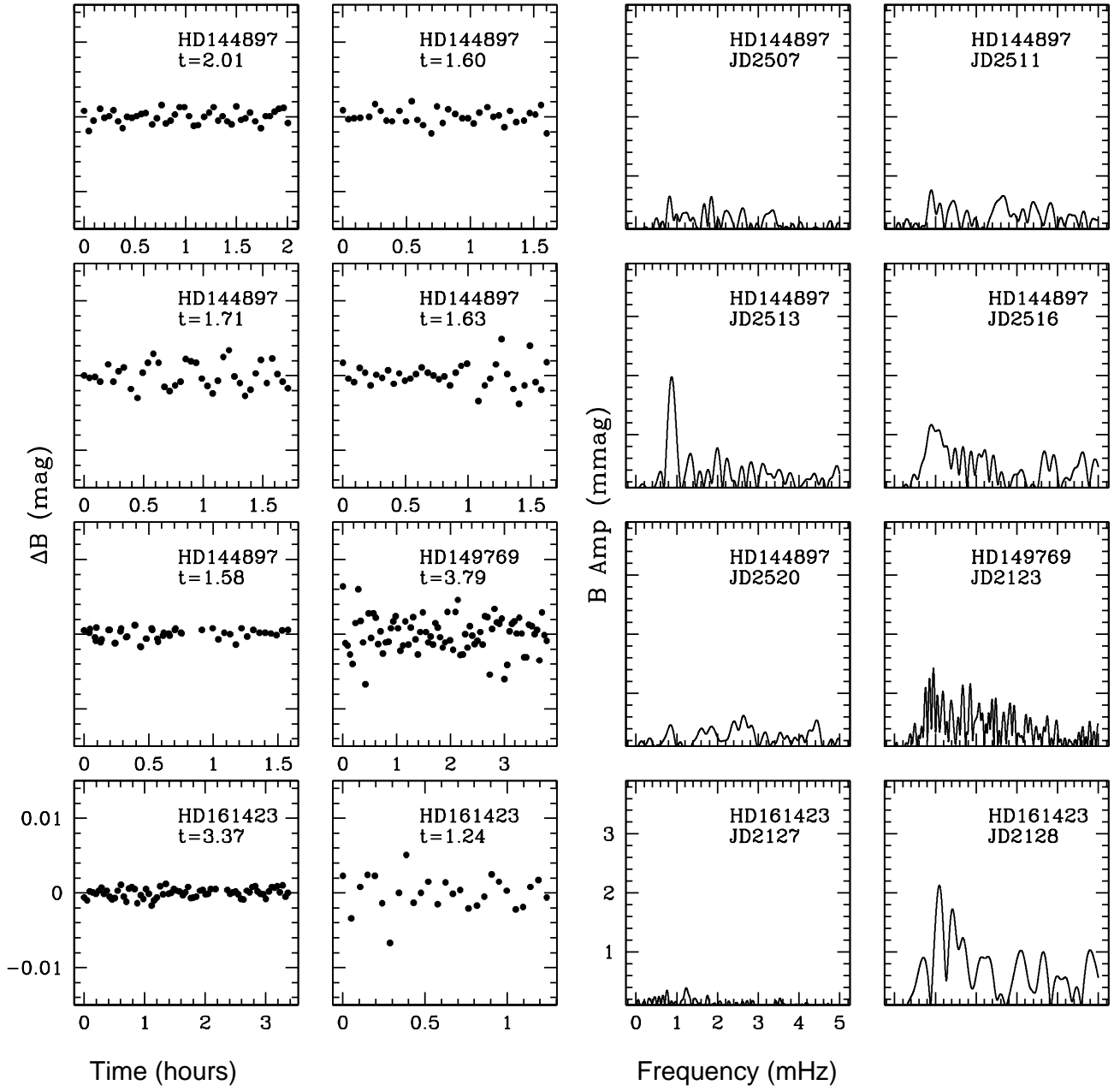


Fig. 3. Continued.

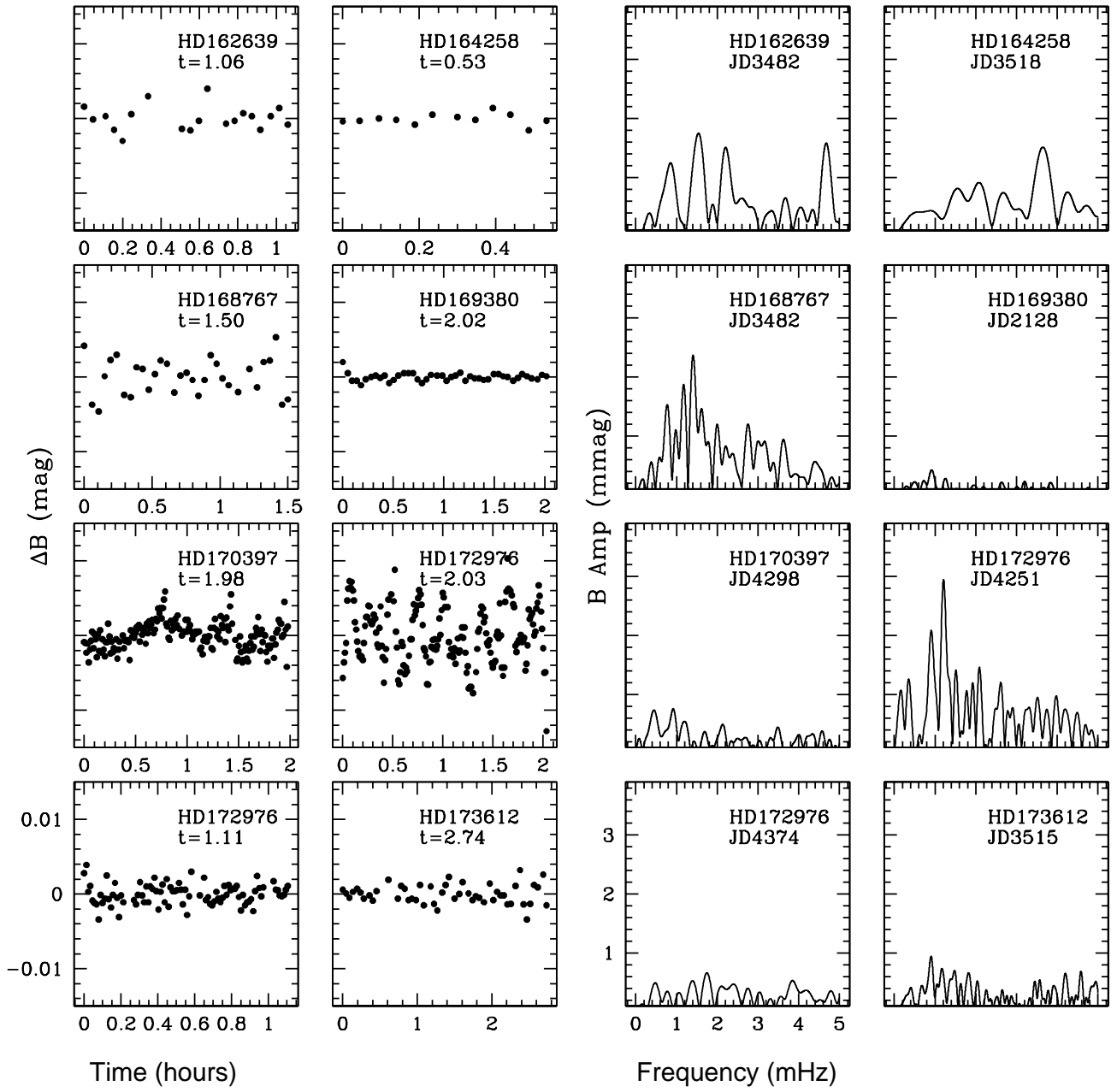


Fig. 3. Continued.

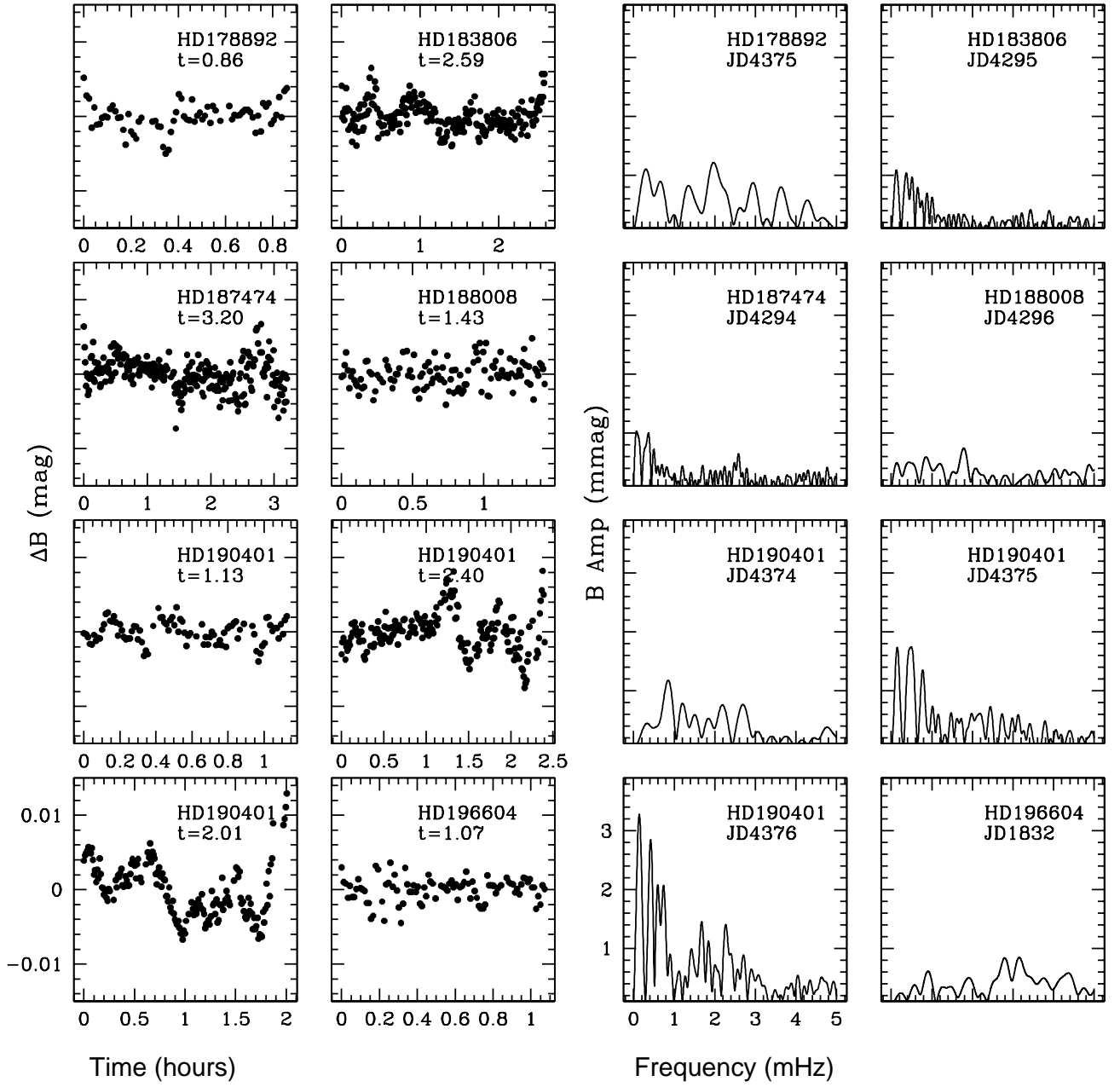


Fig. 3. Continued.

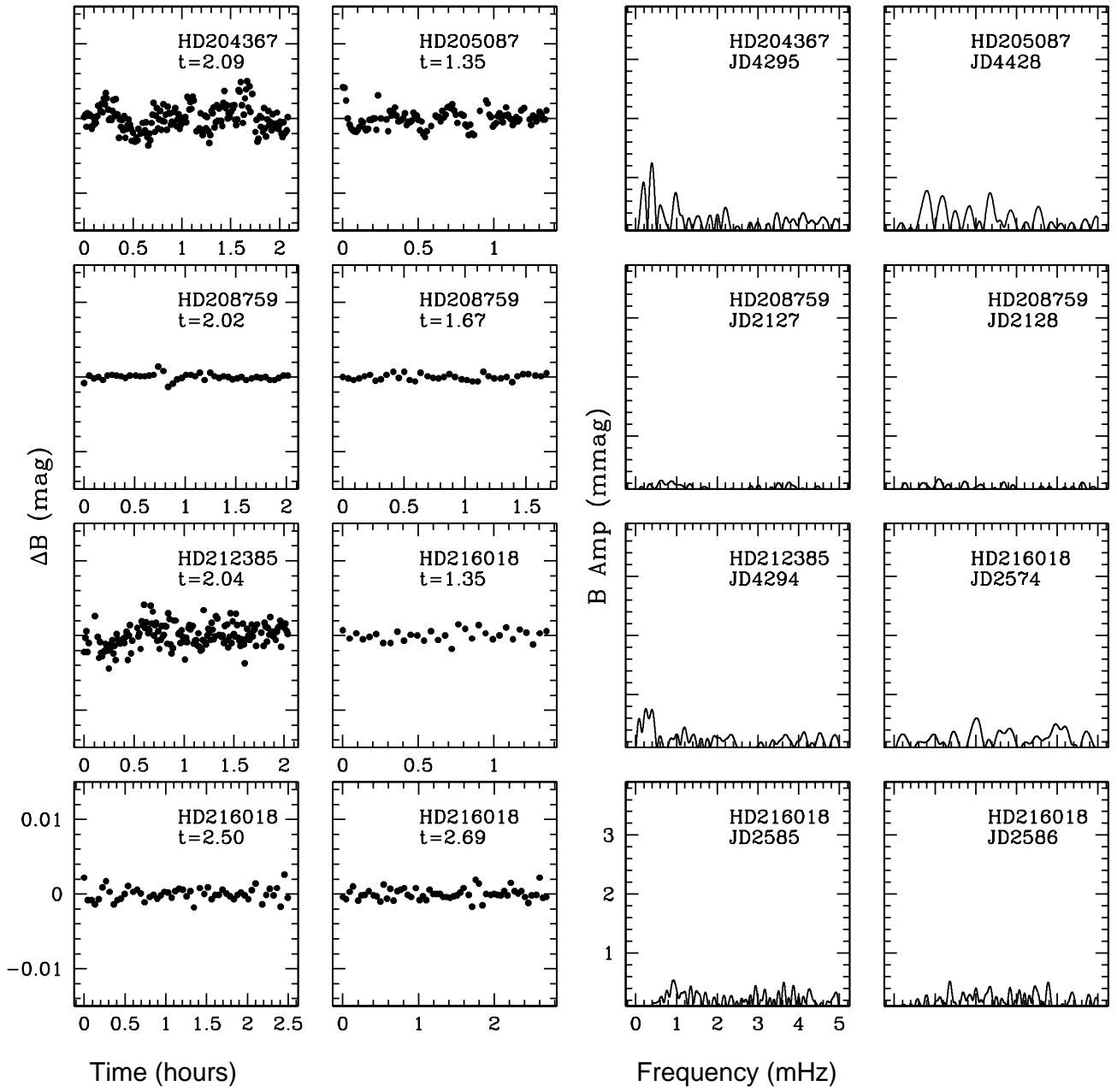


Fig. 3. Continued.

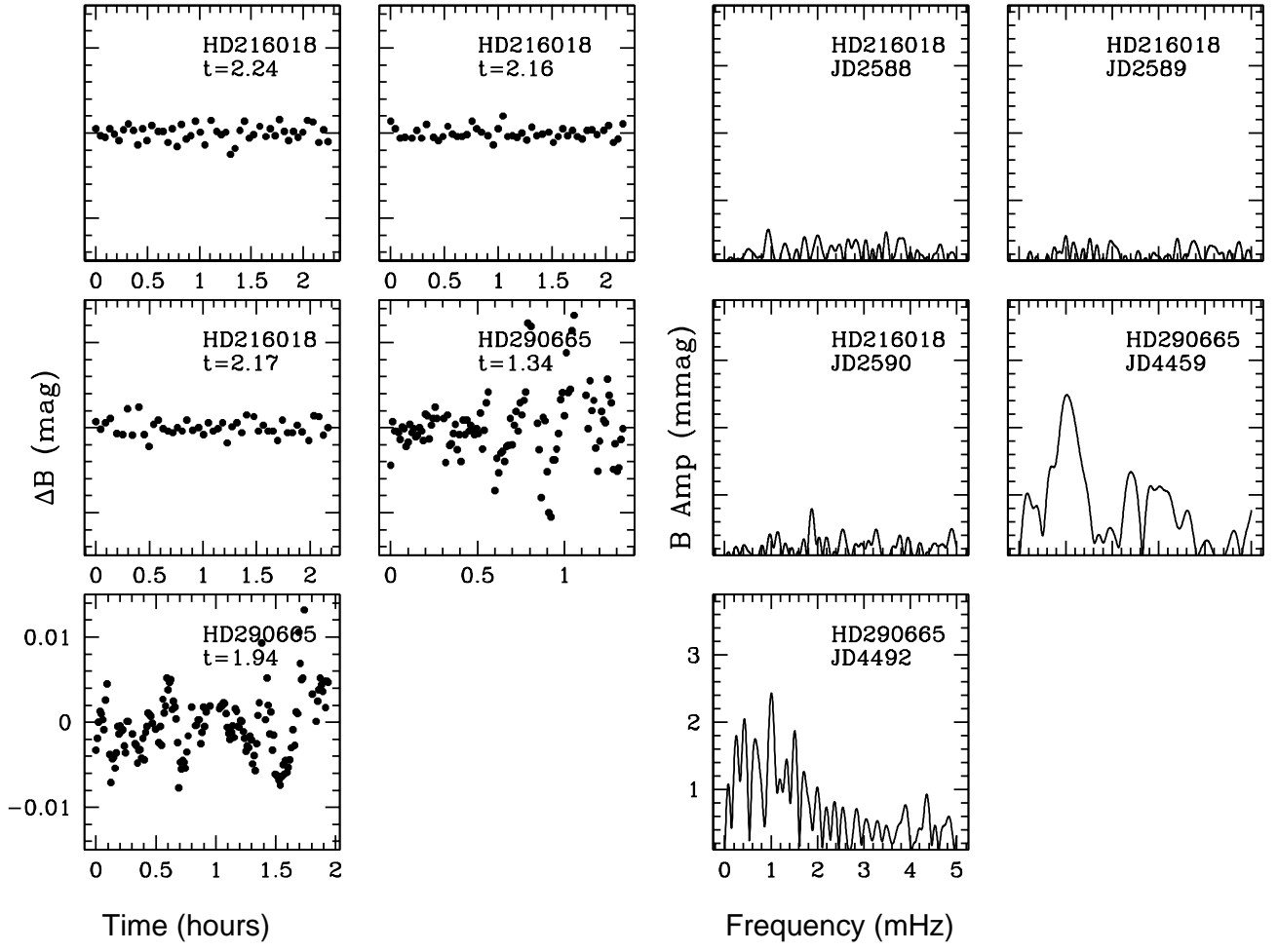


Fig. 3. Continued.

